Electronic-geometric relationships in copper-oxide-based superconductors

Jeremy K. Burdett and Gururaj V. Kulkarni
Department of Chemistry and James Franck Institute, The University of Chicago, Chicago, Illinois 60637
(Received 2 February 1989)

By using orbital ideas linking the dependence of the energies of the d levels at copper sites with the details of the local coordination geometry it is shown through the use of tight-binding theory how the geometrical structure is crucial to the understanding of the electronic structure of copper-containing superconductors. Four systems are studied, the so-called 1:2:3, 1:2:4, 2:1:4, and 2:2:1:3 materials, from the viewpoint that superconductivity is only a possibility if the half-filled band situation at Cu^{II} is destroyed by electron transfer. In the 2:1:4 compound this occurs largely via doping with, e.g., Sr. Here, we also examine the orthorhombic-to-tetragonal distortion of this compound and show by calculation how the driving force away from tetragonal decreases with strontium doping in accord with experiment. We show how this may be interpreted in terms of the changes in chemical bonding as the x^2-y^2 band begins to empty. The 1:2:3 compound is more complex, but an orbital model is developed to follow the change in Cu^{II} charge density with both oxygen stoichiometry in $YBa_2Cu_3O_{7-\delta}$ and also the geometrical changes with temperature and stoichiometry. The focus is on the details of electron transfer to the Cu^{III} chains. As indicated by tight-binding calculations, the relative placement of the x^2-y^2 bands of Cu^{II} and the z^2-y^2 band of Cu^{III} is a sensitive function of the Cu-O distance and the puckering of the $Cu^{II}O^2$ sheets. For $\delta=0$ in the observed structure, the two bands overlap such that charge transfer to the chains is allowed, but at the same time the integrity of the two types of copper atoms is maintained as Cu^{II} and Cu^{III}. For $\delta=0$ in the idealized structure where the planes are not puckered and all Cu-O distances are set equal, the two bands overlap so much that this integrity is lost. For $\delta\sim0.6$, after the c-axis anomaly has shortened the Cu(1)-O(1) distance, charge transfer is completely switched off. At this point T_c is seen experimentally to rapidly drop. Our major finding is that the details of the electronic structure are crucially dependent upon the geometry. We show how the puckering of the $Cu^{II}O_2$ sheets has similar orbital origins to the tetragonal-to-orthorhombic distortion of the 2:1:4 compound. Some structural alternatives are examined for the 1:2:3 stoichiometry using similar ideas. $KY_2Cu_3O_7$ and $AgLa_2Cu_3O_7$ might be possible synthetic goals for a material with the same stoichiometry as the 1:2:3 compound but with a different structure. For the 1:2:4 compound $YBa_2Cu_4O_8$, which contains double chains in place of the single chains found in the 1:2:3 system, some of the copper atoms have to have nonintegral oxidation states. We show that a striking feature of the electronic structure is how the geometry of the system naturally allows such a process to happen. The recently made material $Pb_2Sr_2(R_{1-y}M^{II}_y)Cu_3O_{8+x}$ (2:2:1:3) (R is defined as one of the lanthanide elements and M^{II} is a divalent metal) exhibits structural-electronic features found in the 1:2:3 and in the 2:1:4 systems. Using the simple electronic ideas developed earlier it is suggested that there may be two regions where superconductivity should be observed, one for low and one for high x.

I. INTRODUCTION

The series of high-T_c copper-containing oxide superconductors that have been synthesized and characterized over the past two years[1-7] have provided us with an almost unparalleled set of structures with which to eventually uncover the basis for their astonishing electronic properties. One of the important steps in this direction is associated with understanding the factors which control some of the geometrical aspects of these interesting structures, and how the electronic band structure using a simple tight-binding model is sensitive to them. (A second step towards the understanding of the normal conducting state of these materials is then the addition of many-body effects to such a basic one-electron picture). We have been encouraged in this venture by progress made by chemists in recent years in the understanding of the structures of many solid-state materials using tight-binding theory.[8-10] While certainly not the method of choice for the identification of the lowest energy geometry for an atomic collection of given stoichiometry, it has proven very useful for following changes in relative stability with electron count and identifying features which may stabilize a particular geometry. In qualitative terms of course, it has long provided a framework upon which to develop bonding ideas for solids. At present it is perhaps the most sophisticated approach to structural energetics which is tractable for these complex materials. The present series of compounds are particularly interesting in that the variation in T_c as the composition is systematically changed is now firmly established for two series.

In this paper we will study, using tight-binding theory, several aspects of the electronic control of the geometry of some of these materials, recognizing that the bond lengths and angles associated with the many linkages

shape in a direct way the form of the electronic density of states of the system, and presumably the superconducting properties of these systems. It is interesting that there exist already correlations[11,12] between T_c and the mean Cu-O distance (or the related Cu-Cu distance), and with the average electronegativity of the other atoms present in the solid, two indications that the nuances of chemical bonding are important in controlling T_c. We stress at this early stage, however, that a detailed understanding of the properties of these materials will only come about by the addition of the many-body part of the problem to this simple one-electron description. There have, of course, been several band structure and related calculations on these superconductors (for example, see Refs. 13–27), but those described here will cover a wider spectrum of materials and distortion modes and structural alternatives. What we will show is that the details of the form of the electronic density of states, and the way the bands are filled with electrons, is crucially dependent on the structure.

The version of tight-binding theory that we will use requires solution of the secular determinant $|\mathbf{H}(\mathbf{k})-\mathbf{S}(\mathbf{k})E|=0$, where $\mathbf{H}(\mathbf{k})$ and $\mathbf{S}(\mathbf{k})$ are the Hamiltonian and overlap matrices, using the extended Hückel formalism.[28] The S_{ij} are evaluated directly from atomic wave functions (Slater-type orbitals) and the H_{ij} evaluated using one of the Mulliken approximations $H_{ij}=0.5KS_{ij}(H_{ii}+H_{jj})$ with $K=1.75$. The H_{ii} themselves are estimated from atomic spectral data. The results we will describe below come from such complete tight-binding calculations involving copper 4*s*, 4*p*, and 3*d* orbitals and oxygen 2*s* and 2*p* orbitals (the parameters are given in the Appendix) without the assumption of basis-set orthogonality. [That is, the common approximation $S_{ij}=\delta_{ij}$ is not used in $\mathbf{S}(\mathbf{k})$.] Such an implementation of tight-binding theory naturally includes, therefore, interactions, not only between metal and oxygen orbitals, but those between metal and metal and between oxygen and oxygen. In general, interactions between all pairs of orbitals separated by less than three unit cell measures are included. Beyond these distances direct overlap is generally negligible for the structures we will study. Of course, formally left out of our calculations are all of the many-body effects, which we know are important energetically. However, such simple models have been very useful in the past to view a whole range of systems. If we realize that the (ill-defined) *one-electron* Hamiltonian of the model actually contains corrections for some of the many-body terms left out of the formal model, then its success is a little easier to understand.

In Sec. II we will examine in a general fashion the structural chemistry and *d*-orbital energy level patterns for various copper oxide geometries. In Sec. III these ideas are used to generate the band structure of the 1:2:3 compound as a function of the geometrical variables of the structure. The power of the method comes to the fore here as the influence of distortions, vacancies, and the "*c*-axis anomaly" are readily examined. Section IV derives some structural alternatives for the 1:2:3 compound and includes a discussion of the electron limitations associated with each. Section V examines a related structure, that of the 1:2:4 compound. Section VI examines the orthorhombic-to-tetragonal distortion of the 2:1:4 compound, and shows the importance of electronic effects here, and Sec. VII applies the ideas generated for these superconductors to the recently discovered 2:2:1:3 compound.

II. ENERGY LEVELS IN COPPER OXIDES

In this article we shall be largely interested in the energy levels and bands associated with the copper 3*d* and oxygen 2*p* orbitals of these fascinating systems. The bandwidth clearly plays an important role in controlling the occurrence of the metallic state, and the relative energetic location of the different bands controls their electronic occupancy. The focus will be the relationship between these parameters and the geometrical structure of the system. The structural chemistry of copper is probably unique amongst the elements of the periodic table. It is true to say that its enormous diversity is associated with its position at the end of the transition-metal series such that its structural chemistry reflects aspects of transition-metal chemistry, main-group chemistry, and features which are not observed in either. One of the striking features of the structural chemistry of Cu^{II} is the considerable plasticity of its coordination shell.[29] Thus, there is a continuous progression, exemplified by a series of complexes and extended solid-state arrays, from a regular octahedral geometry to one where two *trans* ligands are missing (the square-planar geometry). Other variants of this are found, from square pyramids containing relatively short, to quite long, distances from metal to apical atom. Such structural effects are often lumped together as "Jahn-Teller" distortions, although on closer inspection this label is not always strictly applicable.[30]

From a chemical point of view the electronic structure of these materials may be built up by consideration of the energy levels associated with local coordination geometries. We will see that this provides a very useful aid in understanding the level shifts of the bands themselves as the structure is changed. Through-bond coupling in oxides is generally considerably smaller than in sulfides. This means that in perovskites,[31] for example, with octahedral coordination of one of the metal atoms, distinct t_{2g} and e_g bands are found. (Sometimes of course they may overlap a bit.) Although, as described above, our numerical results are obtained by allowing interactions between several different types of orbitals, simple perturbation theory ideas are useful in understanding their geometrical dependence.[32] For two orbitals i,j separated in energy by ΔE, the energy shift $\Delta\varepsilon$ on interaction is given to second order by $H_{ij}^2/\Delta E$. Traditionally the interaction integral H_{ij} is set proportional to the overlap integral S_{ij} between the two orbitals as described above. This integral depends upon the distance r between the two centers holding the orbitals i,j and also their angular orientation (θ,ϕ) such that $S_{ij}=\sum_\lambda S_\lambda(r)f(\theta,\phi,\lambda)$ where λ represents the angular momentum components associated with the chemical ideas of σ, π, and δ interactions. The functional dependence of $S_\lambda(r)$ depends upon the details of the atomic wave functions $|i\rangle$, $|j\rangle$, but the

$f(\theta,\phi,\lambda)$ are readily determined from the spherical harmonics themselves and are tabulated in several places.[32] If, because of the geometry of the problem, σ and π bonding are separable and δ interactions precluded by symmetry, as they are in the instances we shall discuss, then we may introduce an energy parameter e_λ to describe a particular interaction and write $\Delta\varepsilon_\lambda \propto S_\lambda^2(r)f^2(\theta',\phi',\lambda)$, which leads to $\Delta\varepsilon_\lambda = e_\lambda(r)f^2(\theta',\phi',\lambda)$ for a specific orientation (θ',ϕ') and for the two cases of $\lambda=\sigma,\pi$. This approach has been termed[32,33] the angular overlap method because of its strong reliance on the ready identification of the form of the angular part of H_{ij}. In the spirit of second-order perturbation theory the total interaction energy between, for example, a central transition metal orbital and a set of ligand orbitals is then given by a sum of such terms and the interaction energy $\Delta\varepsilon$ written in terms of units of e_λ. Now we know that the interaction between metal and oxygen level is strong, and so in a strict sense just adopting the leading term in a perturbation expression is not going to be particularly accurate here. However, we shall find that the *qualitative* use of such an approach is very useful in understanding the electronic structure of these materials. The quantitative details come of course from the numerical calculations themselves.

Figure 1 shows pictorially the form of the $f(\theta',\phi',\lambda)$ for transition metal-oxygen σ and π interactions for the geometrical situations we shall encounter, and Fig. 2 the evaluation of the energies of the transition-metal d orbitals as a result of such a summation. The energy scale is in units of e_λ, and since σ bonding is generally more energetically important than π bonding, $e_\sigma > e_\pi$. It should be remembered too that these parameters depend upon the internuclear separation. In general terms, over the region associated with chemical bonding distances, they increase in magnitude as the distance becomes shorter. Thus, of interest to us later, the x^2-y^2 orbital (actually in the axis system chosen for the 1:2:3 compounds this will be the z^2-y^2 orbital) in a square-planar geometry with short Cu-O distances will lie higher in energy than the x^2-y^2 orbital in a square- or square-pyramidal geometry with longer Cu-O distances. As the details of the geometry change the relative energetic placement of these two orbitals will also change, but in a predictable fashion. Notice too the drop in the energy of the z^2 orbital either as a single atom or as a pair of *trans* atoms are removed from the octahedron. This is a direct result of the loss of antibonding interaction of the atoms involved with the large lobe(s) of z^2. The energy levels associated with the T-shaped unit is a little more complex to evaluate since, because of the lower symmetry, two d orbitals mix together. The method of tackling such problems is described elsewhere.[32] Shown in Fig. 3 is the effect of moving the metal atom out of the plane of four ligands to convert a four-coordinate square geometry into a tetragonal pyramidal one, or to give a five-coordinate square-pyramidal structure an apical-basal angle (ξ) greater than 90°. (We just show the energy changes associated with the highest two orbitals.) The result is a drop in energy of the x^2-y^2 orbital in both cases. Quantitatively this is easy to evaluate; the angular dependence of σ overlap with a lobe of the x^2-y^2 orbitals is $(\sqrt{3}/2)\sin^2(\xi)$. Arguments such as these will be very useful to us when we examine the form of the electronic densities of states computed for these copper oxide structures.

This d-orbital-only model is of course a simplification. In the square-planar geometry the z^2-orbital may mix with the transition-metal 4s orbital, resulting in a stabilization of the former.[34] In molecular Pt^{II} complexes this has been estimated[35] as being worth e_σ. A similar stabilization takes place in the square-pyramidal geometry, but

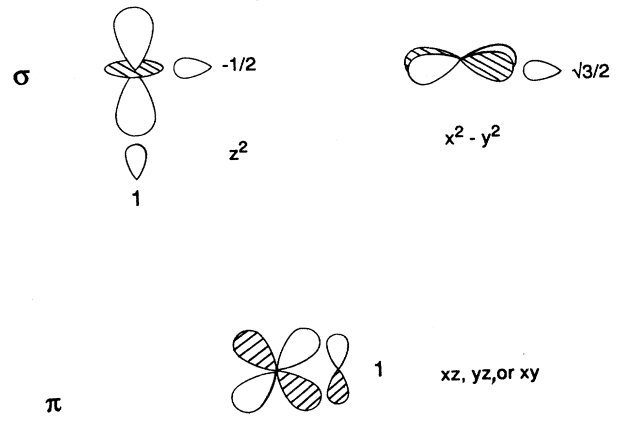

FIG. 1. The $f(\theta',\phi',\lambda)$ of the angular overlap model for σ and π-type interactions with metal d orbitals.

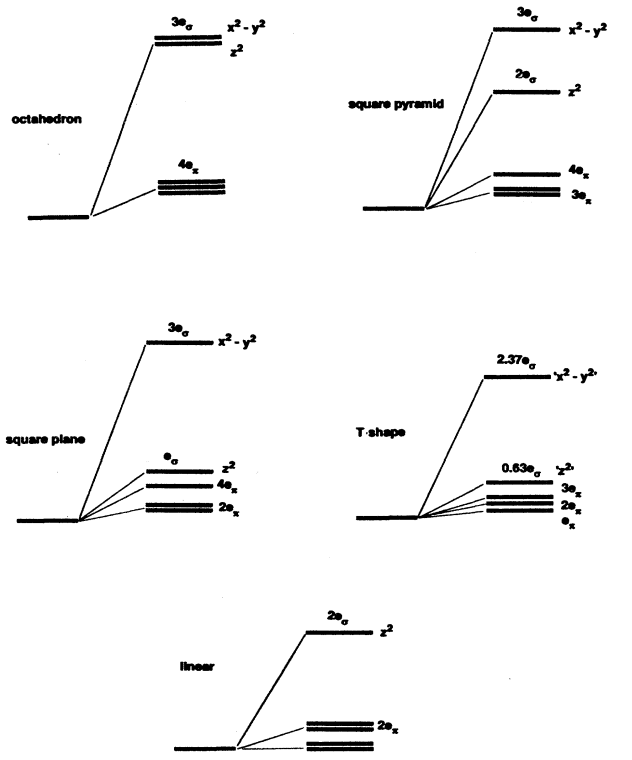

FIG. 2. Angular overlap energy level diagrams for five different coordination environments imporrant in these materials.

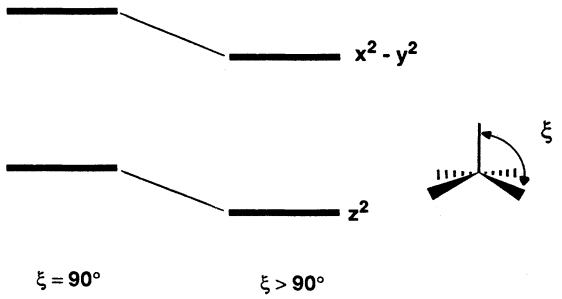

FIG. 3. Schematic variation in energy of the two highest energy orbitals, either of the square pyramid or the square plane, as the axial-basal angle ξ is changed.

here is associated with both $4s$ and $4p_z$ orbitals. An admixture of z^2 and s orbitals has been suggested[30,36] as the feature which determines the almost universal Jahn-Teller distortion of octahedral complexes of two long and four short metal-ligand distances rather than a distortion in the opposite sense. In some square planar *molecular* complexes of Pt^{II} spectroscopic results have indicated[37] that the z^2 orbital lies deeper in energy than the π-type orbitals of the system. Thus we can anticipate that for a nonoctahedral d^9 Cu^{II} system, where the highest occupied band will certainly be that associated with the x^2-y^2 orbital, the next highest could either be a π-type band or that derived from the z^2 orbital depending on the geometry. In the solid these levels will be broadened into bands and their width will depend upon similar overlap considerations. The question of the $4s$ and $4p$ orbitals is an interesting one for the structures and properties of solids. Their interactions in molecules are extremely important,[34,38] and range from determining the nuances of structural and kinetic problems of transition-metal complexes to the intensities of d-d spectral transitions. In the solid state the importance of such higher energy orbitals has been already recognized in studies of the structures of the elemental transition metals, for example.

III. THE 1:2:3 COMPOUND $YBa_2Cu_3O_{7-\delta}$

Electronic structure

The crystal structure of the 1:2:3 compound, the first 90 K superconductor,[2] $YBa_2Cu_3O_{7-\delta}$ (where $0 \leq \delta \leq 1$) is shown[39] in Fig. 4. We show two views that emphasize different features of the structure. We shall use in this paper several different styles of picture to highlight these various points, since the details of the structure will be very important to us. The basic geometrical arrangement, by now well established, is simply derived from the perovskite structure by the omission of some of the oxygen atoms. The hypothetical defect-free perovskite would have the formula $YBa_2Cu_3O_9$. Such defect perovskites are in fact quite well known. We, for example, have already studied theoretically[31] the ordering patterns in the material $Ca_3Mn_3O_{7.5}$ (i.e., $CaMnO_{2.5}$), which may be generated by heating the parent perovskite $CaMnO_3$. The building block in $CaMnO_{2.5}$ is the square

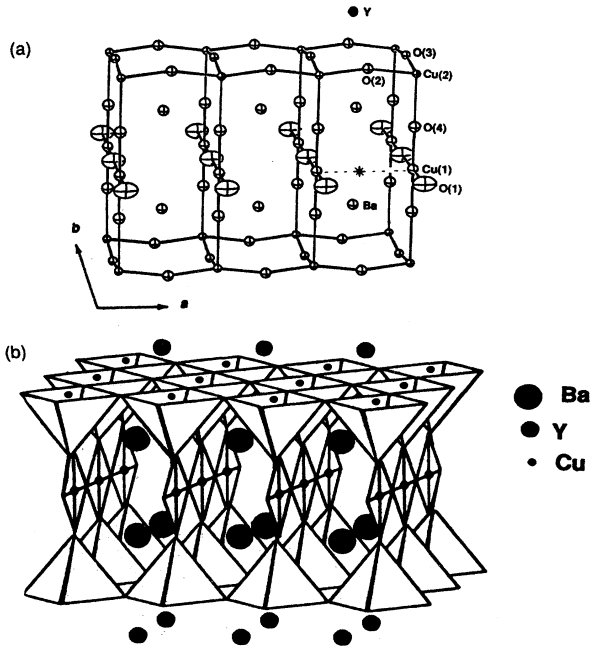

FIG. 4. Two views of the 1:2:3 structure, $YBa_2Cu_3O_{7-\delta}$ with $\delta=0$. In (a) the site called O(5) in the text, and partially occupied for systems with $\delta > 0$, is labeled with an asterisk (*).

pyramid. In the 1:2:3 compound there are square planes and square pyramids. T_c varies[40] with oxygen stoichiometry in a most interesting way (see Diagram 1).

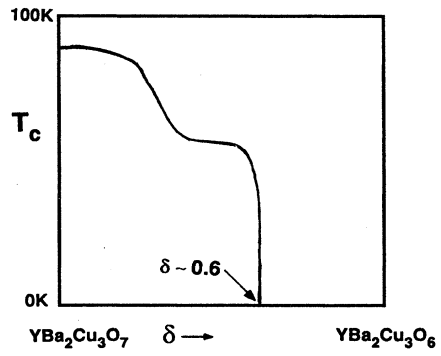

1

For low δ it appears to be almost flat. There then follows another plateau region before T_c rapidly drops.

A question that needs to be answered is why for $\delta=0$ are the vacancies ordered in this particular way. Later we will examine some possible alternative structures. Assignment of oxidation states,[11] formal labels used by chemists to keep track of electrons, is a useful first step. To help us we know that certain geometries are often associated with particular electronic configurations. Square-planar coordination is a geometry always found for low-spin (diamagnetic) d^8 systems (for example Cu^{III}) but occasionally for d^9 systems (for example Cu^{II}). Square-pyramidal arrangements are typical of d^9 systems (for example Cu^{II}). Linear, two coordination is typical for d^{10} systems (for example, Cu^{I}). The T-shaped

geometry, important in our discussions for $\delta > 1$, is a very uncommon one. It is found[41] in a single molecular Rh-containing complex with a low-spin d^8 configuration, where it can be understood theoretically.[32] Here the angle at the top of the T is 154° rather than the 180° expected for the idealized geometry. For copper it is so unheard of that one researcher[42] has termed it an "abnormal" geometry. For Cu^I the known three-coordinate geometry closest to the T shape is probably the distorted triagonal plane found[43] in the series of cyanide complexes $KCu_x(CN)_y$ where $x = 1,2$ and $y = 2,3$.

In $YBa_2Cu_3O_{7-\delta}$ for $\delta = 0$, diffraction studies have shown that the site labeled O(5) is empty, and so using this correlation between oxidation state and local geometry, the following picture emerges. The structure consists of $Cu^{II}(2)O_2$ sheets linked by rather long Cu(2)-O(4) linkages to $Cu^{III}(1)O_3$ chains. The sheets thus contain roughly square-pyramidal Cu^{II} atoms while the chains contain Cu^{III} atoms in approximately square-planar coordination, leading overall to an orthorhombic structure (*Pmmm*). For $\delta = 1$, all of the atoms labeled as O(1,5) are missing, the square planes have been replaced by linear O-Cu^I-O dumbbells, and now the structure is tetragonal (*P4/mmm*).

Such a viewpoint is confirmed by the correlation between the computed band structure and the qualitative picture that we would get by using the ideas of the previous section. Figure 5 shows how the orbital diagrams associated with these local units get broadened into bands in the extended solid. Since the electronic area of interest lies between d^8 and d^{10} we shall concentrate on the behavior of the x^2-y^2 and z^2-y^2 bands. There are twice as many x^2-y^2 levels as there are z^2-y^2 levels, reflecting the stoichiometry of the material. In pictures of this type we will generally indicate the relative numbers of levels via the width of the box depicting the band. The picture that results shows two half-full bands corresponding to x^2-y^2 orbitals on the two Cu^{II} atoms, and an empty z^2-y^2 band

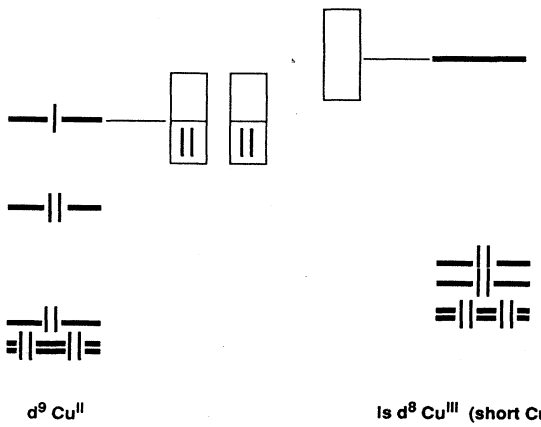

FIG. 5. Broadening of the levels of local fragments into energy bands in the expected solid for the 1:2:3 structure. Only the two highest levels are shown.

on the Cu^{III} atom. (This is a simplification we use for now. It will be slightly, but crucially, modified later.) This z^2-y^2 label is simply an x^2-y^2 orbital in a different orientation. Notice that the z^2-y^2 band associated with the chain atoms lies to higher energy than the x^2-y^2 band associated with the plane atoms. This is a natural consequence of the shorter average Cu-O distance in the chains compared to the planes which gives rise to a larger value of e_σ for the former. If the Cu(1)-O distances were the same as the Cu(2)-O distances the two bands would occupy very similar energetic positions. There is an important observation concerning the symbiosis of electronic and geometrical effects in the structure. The way the atoms are connected in this arrangement allows structural flexibility for the chain atom coordination in the sense that the Cu(1)-O(4) distance is not fixed by the coordination demands of other atoms. It is able to adjust to such a length that the z^2-y^2 band lies to higher energy than the x^2-y^2 bands, and so preserve the Cu^{II} and Cu^{III} labels. We will see a similar effect below when discussing pyramidalization at Cu^{II} in the observed and possible alternative structures for this stoichiometry.

The bandwidths and energetic location of the bands from our calculations are somewhat different from those found from other methods. This is a typical result of one-electron calculations of this type, both in molecular and solid-state areas. We have made no attempt to parametrize our calculations to mimic the results of numerically much-better ones. Experience tells us that the basic ideas concerning the electronic structure and how it changes on distortion will be similar, since so many of the details of the band structure are controlled by symmetry, overlap, and electronegativity differences between the basis orbitals of the problem. The *numerical* details of bandwidth and location may well be somewhat different, but unless we want to compare them with experiment (which we do not in general), these differences will not be important in those geometrical aspects of the structure we wish to study.

The oxidation state formalism and these *d*-orbital labels have been used to describe these energy bands. As we have noted the former is just a way of keeping track of electrons; we do not mean that the charge on the metal is +2 for a Cu^{II} atom. Neither does the description of such a species as a d^9 system imply a similar charge distribution. It does, however, allow us to understand the placement of electrons in energy levels and bands very well. Similarly when describing these energy levels and bands as x^2-y^2 or z^2 these are useful labels; we do not imply that these orbitals contain 100% metal character. As we have noted earlier they are heavily mixed with other orbitals, and it is quite possible that the oxygen contribution is the larger one. Sleight has emphasized the correct "chemical" use of these labels elsewhere.[11,12]

Orbital description

This question of orbital description is an interesting one, and one which is strongly dependent on the location of the level in the band (or rather the point in **k** space).

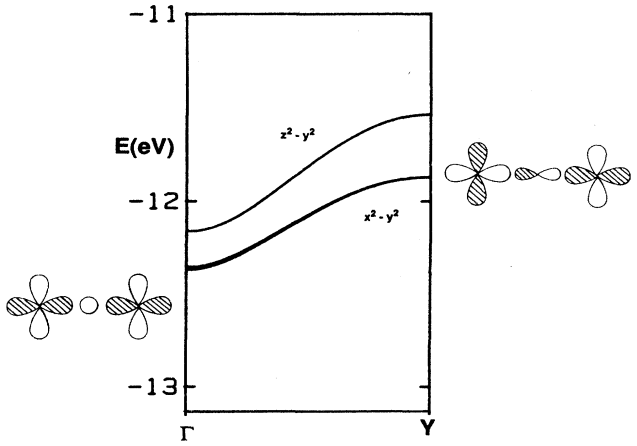

FIG. 6. Dispersion along one of the symmetry directions of the Brillouin zone of the three highest energy bands of the valence shell. There are two x^2-y^2 bands, shown with the thicker line, one symmetric and the other antisymmetric with respect to the mirror plane which runs through the Cu(1) atoms. A generic orbital description of one sheet of these x^2-y^2 bands is shown.

Figure 6 shows the dispersion behavior of several of the energy bands along one of the symmetry directions. The energetic behavior and description is simplified because the $\cdots$O-Cu-O-Cu$\cdots$ linkages run in perpendicular directions, and in the idealized structure where there is no sheet puckering, all angles are either 90° or 180°. There are two, nearly degenerate x^2-y^2 bands for the square pyramidal Cu(2) atoms. These two bands are respectively symmetric and antisymmetric with respect to the mirror plane passing through the central copper atom Cu(1). Notice that the bottom of each band lies at the zone center, and, if the axial-basal angle of the square pyramid is 90°, involves by symmetry the antibonding interaction between the metal x^2-y^2 orbital and the oxygen 2s orbital located on the atoms in the planes. The top of the band lies at the zone edge and involves by symmetry the antibonding interaction between the metal x^2-y^2 orbital and the oxygen $2p\sigma$ orbital lying in the planes. (There are too contributions from copper 4s and 4p orbitals respectively at these two points in the zone.) Decreasing the metal-oxygen distance will result in larger interactions of both types, and the mean band position will move to higher energy. Since the interaction with oxygen 2p is larger than that with 2s (understood via second-order perturbation theory arguments), the width of the band will increase with decreasing distance. It is interesting to see how the symmetric and antisymmetric bands split apart in energy. If $a = b$ and the axial-basal angle of the square pyramid is 90° then by symmetry there can be no coupling between the two metal x^2-y^2 orbitals as has been mentioned elsewhere.[27] However, in the real structure there is an asymmetry between a and b and the x^2-y^2 orbital mixes with the 4s orbital on the same atom. Now, as shown in Diagram 2

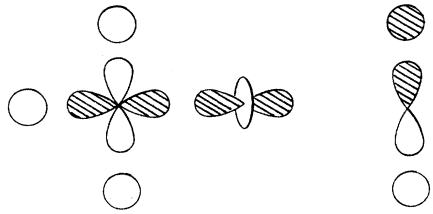

2

the x^2-y^2 orbitals on Cu(2) may couple through symmetric (s, x^2, and z^2-y^2) and antisymmetric p orbitals on Cu(1). Our calculations show, however, that the effect is actually quite small.

As we will see later the puckering of the sheets in the 1:2:3 compound is very important. The change in the form of the wave function on puckering is quite striking. An admixture of p_z character into the oxygen orbital contribution rapidly becomes important, as shown in Diagram 3.

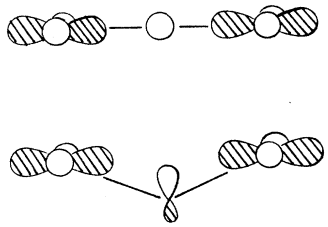

3

On bending this orbital starts to develop some lone-pair character on oxygen.

Distortions of the structure

There are three distortions of the structure which we will examine here. The first is the movement of the square-pyramidal copper atom out of the plane of the basal oxygen atoms to give an apical-basal angle greater than 90° and results in a puckered Cu(2)O_2 sheet. The actual structure is distorted in this way [see Fig. 4(a)] and, as we will see, this plays an important role in controlling charge transfer. The second distortion is the alternate shortening and lengthening of adjacent Cu—O bonds in both directions of the CuO_2 planes: a breathing type of motion which is not found as a static distortion (within experimental error), and may or may not (depending upon the viewpoint) play a crucial part in the superconduction process. The third is the change in a and b, specifically $b - a$, important not only in understanding what happens when the system is cooled, but also when the stoichiometry is changed.

Increasing the apical-basal angle above 90° leads to a reduction in the overlap of the ligand orbitals with the metal x^2-y^2 orbital as shown in Fig. 3. In fact, there is a more complex rehybridization of orbitals which takes place at the metal center and is described in Ref. 34. Since the interaction is an antibonding one, a stabiliza-

tion of these levels results. Our calculations do indeed show a drop in the mean energy of this band [Fig. 7(c)] and a stabilization of the structure as a whole [Fig. 7(a)]. The puckering energetics are also influenced by the bending at oxygen. With a total of eight valence electrons (four pairs) a bent geometry is expected here. However, π bonding stabilizes the linear geometry, and bending at oxygen is often quite soft,[34] leading to, for example in the silicates, a whole range of Si-O-Si angles. For the present discussion the most important electronic result of the puckering is the drop in energy associated with the x^2-y^2 band in accord with the result of Fig. 3. However, we would expect an analogous *destabilization* of the corresponding bonding orbital, such that overall the net effect should be to resist such bending. Since the energetic effect of antibonding orbitals is considerably larger than that associated with their bonding partners as shown schematically in Diagram 4,

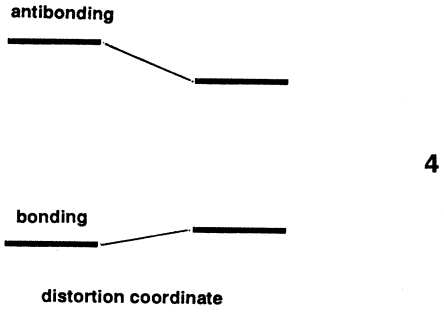

4

one often finds that the energetics associated with distortions of molecules and solids are controlled by the highest occupied levels or bands. (See the discussion in Ref. 34.) This comes about on the present model via the inclusion of overlap in off-diagonal terms in the tight-binding calculation. Similar electronic effects are found in many areas of chemistry. For example pyramidal CX_3 (X=F, Cl, etc.) molecules are found to be contrasted with the planar structure for CH_3. In CX_3 both π-bonding and π-antibonding levels are occupied and the two orbital-four electron destabilization at the planar geometry is alleviated by bending.[34] For CH_3 there are no π-type orbitals. In the copper oxide system the relevant orbitals are of σ type. The prediction of the model Diagram 4 is that as electron density is added to the x^2-y^2 band then the driving force for puckering is increased and a more puckered structure will be found. There are other solid-state examples of the same type. One that involves a π-type interaction is that of the planar or pyramidal geometry at oxygen in the MO_2 structures of rutile (planar) and $CaCl_2$ (pyramidal). The planar structure is found for low electron counts where antibonding orbitals are not occupied, but by the time the π^* levels are full (at d^6) the pyramidal structure (the analog of the puckered structure in the copper oxides) is favored.[44]

Figure 7(b) shows the variation in the total energy on distortion for the 1:2:3 compound for the low-spin d^6 configuration where none of the σ antibonding orbitals are occupied. Thus the observed angle at $d^{8.67}$ is a balance of the two effects, namely the stabilization of x^2-y^2 and the destabilization of the deeper-lying orbitals. A similar electronic picture involving this orbital will be

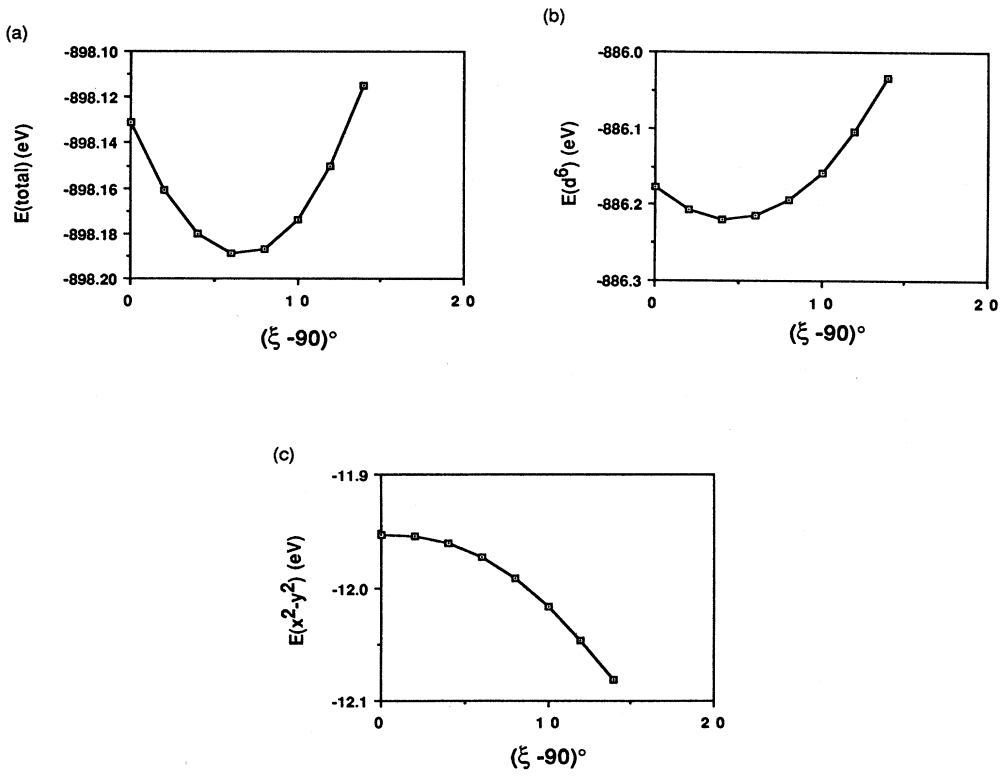

FIG. 7. Energetic changes on puckering the CuO_2 planes of the 1:2:3 structure. (a) Total one-electron energy for $d^{8.67}$. (b) Total one-electron energy for d^6. (c) Orbital energy for x^2-y^2.

found below in the tetragonal-orthorhombic distortion of the 2:1:4 compound, where there is clear experimental evidence to show that the driving force for the distortion is controlled by the occupancy of the x^2-y^2 band. The form of the wave functions changes too as a result of the distortion as we have described above. A calculation that includes the Y atoms reproduces quite well ($\xi_{min}=96.5°$) the observed geometry[39] in the 1:2:3 compound. Here there are two different angles along a and b with an average of $\xi=97.9°$. (We shall examine later the role of the Y orbitals here.) Also in accord with the idea that antibonding interactions are relieved on bending, we find an increase in the Cu—O bond overlap population as the distortion proceeds. In practice a feedback process is at work here which we cannot model accurately. As the distortion away from $\xi=90°$ proceeds this strengthening of the Cu—O bond should result in a shortening of the Cu-O distance. The angle change and bond shortening will work in opposite directions in broadening the x^2-y^2 band. We will return to this distortion in Sec. VIII.

The second distortion, shown in Diagram 5(a),

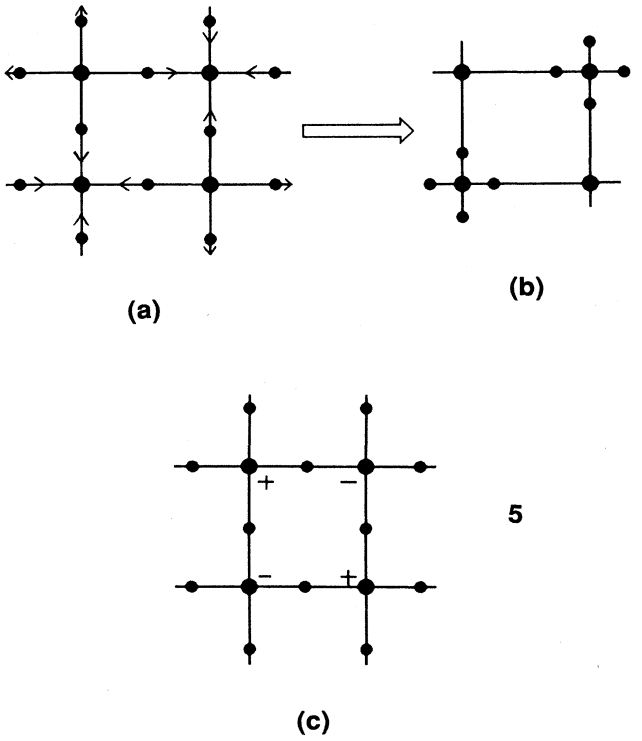

5

and described as a "breathing" motion within the CuO_2 planes, is one which has been associated with the "disproportionation" mechanism of superconductivity favored by many in the chemical community (see, for example, Ref. 45 and the series of articles in Ref. 6). Figure 8 shows how the densities of states associated with the x^2-y^2 bands change under such a motion. As the distances around one copper atom contract, the band A is pushed to higher energy and becomes largely associated with this copper atom. As the distances around the other copper atom expand, the band B moves to lower energy and becomes largely associated with this second type of copper atom. Overall the effect is to transfer electrons

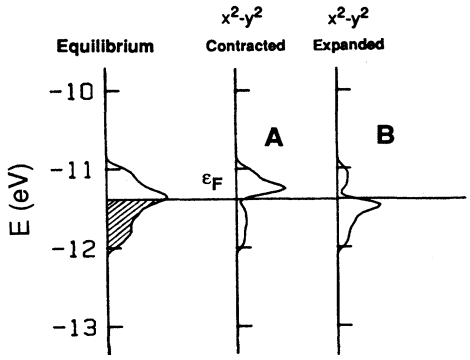

FIG. 8. Changes in the x^2-y^2 densities of states on breathing [Diagram 5(a)].

from A to B, and as a result the copper atom with the shorter Cu-O distances becomes more Cu^{III}-like and the copper atom with the longer Cu-O distances becomes more Cu^{I}-like. There have been suggestions that strong electron-phonon coupling of this type can provide a mechanism for superconductivity. This applies both to the copper-containing systems (where it involves $2Cu^{II}\rightarrow Cu^{I}/Cu^{III}$) and the copper-free system $Ba_{1-x}K_xBiO_3$ (where it involves $2Bi^{IV}\rightarrow Bi^{III}/Bi^{V}$). Increasing and decreasing the Cu-O distances by an amount equal to the magnitude of the thermal vibration parameter associated with the Cu-O distances, determined experimentally from neutron diffraction studies[39] on the 1:2:3 compound, leads to a calculated charge transfer of 0.22 electrons. Notice that although there are two x^2-y^2 bands (the symmetrical-antisymmetric pair) split apart by a small amount in the undistorted structure, there is no charge transfer from one copper atom to another until two geometrically distinct sites are produced via a distortion.

Energetically we find by calculation a stabilization for such a distortion. This is shown in Fig. 9 as a function of d count. Such global pictures are very useful in understanding the origin of such distortions. Using the language of the moments method[46–48] (described in greater detail in Sec. IV) the shape of the curve associated

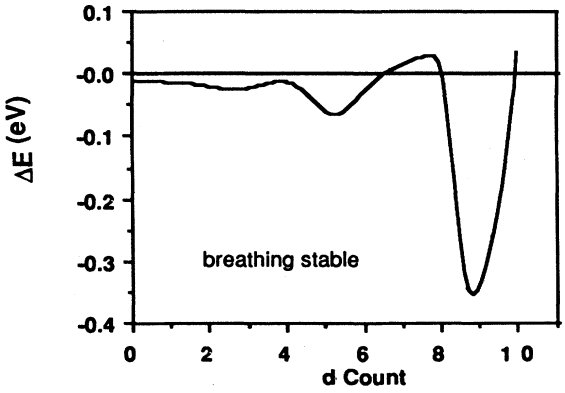

FIG. 9. Computed stabilization energy of the breathing mode [Diagram 5(a)] in the 1:2:3 compound as a function of the average number of d electrons per copper.

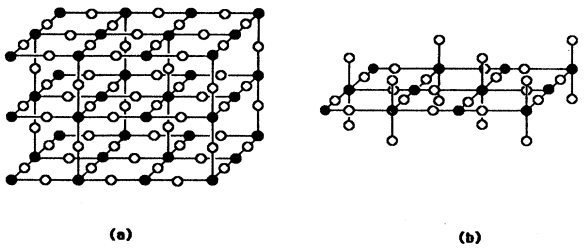

FIG. 10. A hypothetical structure (a) which during a disproportional distortion (b) leads to square-planar Cu^{III} atoms and two-coordinate Cu^{I} atoms.

with d-orbital configurations corresponding to the occupancy of x^2-y^2 and z^2 orbitals is a fourth-moment one, typical of Jahn-Teller and Peierls distortions. Left out of our simple one-electron calculations, however, are the Coulomb terms and these are clearly important in controlling the distortion energetics. In particular the on-site repulsions associated with the two electrons in the x^2-y^2 band of the Cu^{I}-like atoms will destabilize such a distortion. Similar comments apply to other compounds containing sheets of square planar Cu^{II} atoms. The size of these terms are difficult to evaluate. From values of atomic ionization energies[49] the disproportionation reaction $2Cu^{II} \rightarrow Cu^{I}/Cu^{III}$ costs 16.54 eV. For the bismuth case, $2Bi^{IV} \rightarrow Bi^{III}/Bi^{V}$, it costs much less, 4.7 eV. For gold $2Au^{II} \rightarrow Au^{I}/Au^{III}$ the figure is 13.5 eV. Disproportionation is observed both in $BaBiO_3$ and in $CsAuCl_3$ and so these figures need to be modified for use in the solids under consideration. There is a good case to be made that the Cu—O bond is less covalent than the Au—Cl one, and thus the gas-phase figure will be reduced more by chemical bonding in the latter.

There is though another problem with a large amplitude motion of this type in these copper-containing systems. As the breathing distortion proceeds[50] in the $BaBiO_3$ system, one bismuth (Bi^{V}) develops four short Bi-O distances and another (Bi^{III}) four long Cu-O distances. Such a disortion is a perfectly acceptable one since octahedral coordination with these dimensions are known for both of these bismuth oxidation states. However, as the distortion in the CuO_2 plane increases, the geometry of one half of the structure is composed [Diagram 5(b)] of a copper atom with four tightly bound oxygen atoms (clearly Cu^{III}-like) and the other half of a copper atom with four loosely bound oxygen atoms. It is this second arrangement that electronically should be Cu^{I}-like, which we find unlikely for this oxidation state of copper. This observation may argue against a large static disortion of this type. It is thus possible that the large Coulomb U associated with such a disproportionation has a structural component too. (Our one-electron calculations are not at all good at accurately mimicking the energetics associated with breaking bonds and so we cannot lean on our computed energetics to help us here.) It is not possible to find a distortion that leads to a square-planar Cu^{III} and dumbbell Cu^{I} moities for large amplitude distortions of the 1:2:3 structure. Figure 10 shows an alternative structure where such distortions are possible but this corresponds to a stoichiometry of $(A,B)_3Cu_3O_{8.25}$. Such a species would need a mixture of three- and four-valent ions for A and B. We shall investigate later a structural alternative for the 1:2:4 compound which is not known and contains Cu^{III} and Cu^{I}.

There is an interesting motion, a hybrid of the two which we have described, which also might be important. This is shown in Diagram 5(c). The motion involves movement of the copper atoms only of the sheet, and these move up (labeled with a +) and down (labeled with a −) from their equilibrium positions in a coupled fashion. As the puckering decreases around one site (A) the Cu-O distances to that copper decrease accordingly if the cell dimensions remain unchanged. The converse is true at the other site (B). As far as the relative energies of the x^2-y^2 bands are concerned they look similar to that of Fig. 8 with its A and B labels. The effect is somewhat larger here since the shift in band location is compounded by the effects of bond stretching (contracting) and sheet puckering (flattening). This motion is particularly interesting in that since there is no oxygen atom movement, the oxygen isotope effect associated with it should be zero.

The third distortion we will study is that of changing $(b-a)$. Figure 11 shows the energetic behavior of such a distortion with electron count. Close to the electron counts important for the 1:2:3 compound, the sensitivity

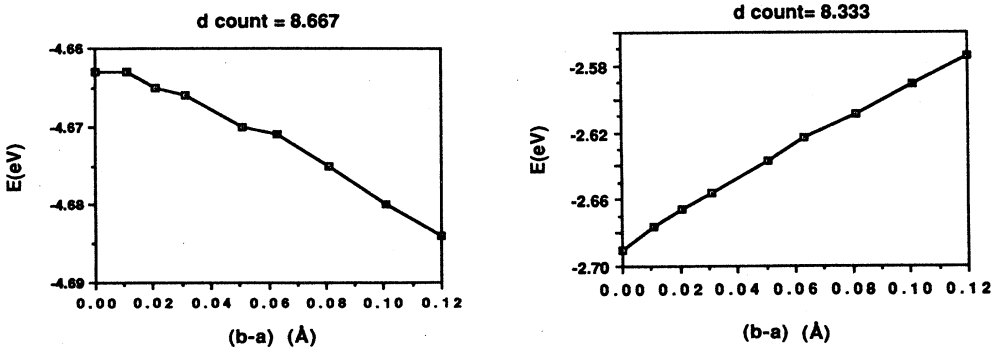

FIG. 11. Computed changes in the stabilization energy associated with increasing $b-a$ for two electron counts.

TABLE I. Parameters used for the calculations.

Atom	Orbital	H_{ii} (eV)	ζ_1[a]	c_1[b]	ζ_2[a]	c_2[b]
O	2*s*	−32.30	2.275			
	2*p*	−14.80	2.275			
Cu	4*s*	−11.40	2.20			
	4*p*	− 6.06	2.20			
	3*d* (Cu^{II})[c]	−14.0	5.95	0.5933	2.30	0.5744
	3*d* (Cu^{III})[c]	−14.6	5.95	0.5933	2.30	0.5744
Y	5*s*	− 8.0	1.60			
	5*p*	− 3.0	1.60			

[a]Slater-type orbital exponents.
[b]Coefficients of a double-ζ expansion.
[c]See text.

of the distortion sharply changes. This is easy to understand. While the x^2-y^2 bands of Cu(2) are filling, the system should be resistant to distortion since there are antibonding interactions with x^2-y^2 along both *a* and *b*. Increasing the antibonding interactions along one direction will more than offset the decrease in antibonding interactions along the other. However, as soon as the Cu(1) z^2-y^2 band starts to fill, such symmetry is lost and electrons are placed in an orbital which is strongly antibonding along the *b* direction. We can therefore understand the calculated stabilization associated with such a distortion. Our one-electron computations are not reliable when it comes to predicting equilibrium bond lengths, and so although we know that larger values of $b-a$ are to be expected when this band starts to fill we do not blindly follow the implication of Fig. 11 that the system will fall apart along *b*.

There is one further important electronic point which influences the distortion energetics. Until now we have avoided the question of the choice of parameters for the calculations. Following our long-standing philosophy we have used standard literature values[32] for the copper and oxygen orbitals. In fact, since there are two different copper atoms, ostensibly Cu^{II} and Cu^{III}, in the structure we should really use deeper-lying atomic parameters for Cu^{III} than for Cu^{II}. Indeed in the real (i.e., observed) geometry for the 1:2:3 compound, use of the same copper parameters for both atoms leads to a computed result where the bottom of the z^2-y^2 band of Cu^{III} lies very close to the half-filled point of the x^2-y^2 band of Cu^{II}, but still above it. Increasing the size of H_{dd} for Cu^{III} relative to that of Cu^{II} leads to the band overlap we describe above and the charge transfer we consider so important. The difference between the two H_{dd} values will be a sensitive function of the charge transfer. Self-consistent charge calculations designed to model this behavior did not converge but the value shown in Table I (see Appendix) is consistent with the computed charge difference between the two copper atoms and the experimental dependence of copper 3*d* ionization potential on charge.[49] The actual electron count at which the sign of the distortion energetics changes (Fig. 11) is on this model sensitive to the choice of H_{dd} parameters for the two copper atoms Cu(1,2). From our calculations as the Cu(1) becomes more electronegative the crossover occurs at lower *d* counts, a result easily understood.

The way the bands change in energy with $b-a$ is interesting. As we have mentioned, the increase in the strength of antibonding interactions along one direction coupled with a decrease in antibonding interactions along the other effectively leads to no change in the width or position of the x^2-y^2 bands of Cu(2). However, increasing *b* will lead to a drop in these parameters for the Cu(1) z^2-y^2 band. Diagram 6

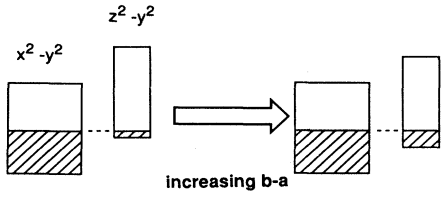

6

shows schematically the change in the calculated density of states for this process, in agreement with our simple model. (Recall that in pictures of this type we will generally indicate the relative numbers of levels via the width of the box depicting the band.) The important result for later use is that the z^2-y^2 band drops in energy with increasing *b*.

Charge transfer between planes and chains

We are now in a position to investigate the question of charge transfer between chains and planes.[51,52] While in the 2:1:4 compound ($La_{2-x}Sr_xCuO_4$) the electron density in the x^2-y^2 bands is broadly controlled by the amount of strontium doping, the corresponding feature in the 1:2:3 compound is determined by the geometrical effects we have described above. The broad brush model we have suggested so far involves two half-filled x^2-y^2 bands located on the Cu^{II} atoms in the planes and an empty z^2-y^2 band associated with the Cu^{III} atom in the chains. In fact the bands overlap sufficiently that electron transfer takes

place from the former to the latter making the Cu^{III} atoms more Cu^{III}-like and the Cu^{II} atoms more Cu^{III}-like (Diagram 7).

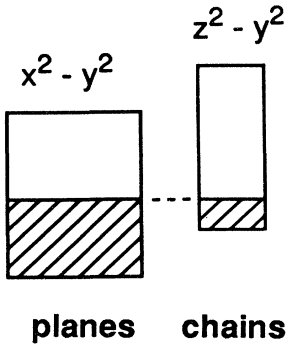

7

This overlap is very important since it removes the possibility of several effects associated with half-filled bands. As the transfer increases, the tendency for the opening of a Hubbard gap, and the tendency for a Peierls distortion or other instability is reduced. Recall, for example, the dramatic change in the energetics of the distortion shown in Fig. 9 on moving away from the $d^{8.667}$ configuration corresponding to a half-filled x^2-y^2 band. (A similar effect should pertain for the case where electron transfer *to* the band occurs.) A diamagnetic metallic state is thereby encouraged. Thus on this model the chains play a similar role in the 1:2:3 compound as Sr doping does in the 2:1:4 compound. In $La_{2-x}Sr_xCuO_4$ itself superconductivity is found as x increases past approximately 0.055; i.e., 0.055 electrons are removed from the x^2-y^2 band of the copper. In our simple model then the chain bands must remove a similar amount of electron density from the planes before the 1:2:3 system becomes a superconductor. We note the experimental correlation (see the collation of data in Ref. 42) between T_c and the Cu^{III} content of the superconductor which bears directly on this point. [Parenthetically we draw attention to the report[53] of an increase in Cu(1)-O(4) distance in the 1:2:3 compound around T_c. Since the z^2-y^2 band is Cu(1)-O(4) antibonding, changes in electron density should show up in such changes in bond lengths.] Also, we note[54] the apparently monotonic drop in T_c with zinc doping. Zn^{II} is a d^{10} system, and substitution of Cu(2) by zinc will tend to fill up to half full the x^2-y^2 band, thus eventually switching off the superconductivity. (This occurs for close to 14% zinc.) Crudely assuming equal densities of states for the three bands at the Fermi level, this corresponds to the addition of about 0.043 electrons per Cu(2), a similar figure to that just quoted for the 2:1:4 compound. (This assumes, of course, that the zinc is simply present as a provider of an extra electron compared to copper and does not play a larger role.)

By how just the band overlap changes, and therefore how much electron density is removed, depends crucially on the geometry of the system. We have noted above that the interaction energy between a ligand orbital and a metal d orbital has a well-defined angular dependence. Thus, as the apical-basal O-Cu-O angle increases from 90° (i.e., as the basal atoms of the square pyramid become nonplanar), so the overlap between the two decreases, and the destabilization energy relative to an isolated d orbital energy is reduced. Similarly, as we have described above, with a change in Cu-O distance the center of mass of the band will change. Both geometrical effects can also result in changes in the shape of the band with a further corresponding dependence of the density of states at the Fermi level on geometry.

Figure 12 shows how the calculated electron transfer from the x^2-y^2 bands to the z^2-y^2 band varies with $b-a$ [related to the orthorhombic strain, $(b-a)/(a+b)$] from a series of calculations keeping $a+b$ constant. Lines on the plot show the geometrical parameters associated with room temperature and 100 K structures. Basically the x^2-y^2 bands of the planes remain unchanged in energy since contraction along a, e.g., is matched by a corresponding expansion along b. This is not the case for the z^2-y^2 band in the chains. It is sensitive only to changes along the b direction as we have noted. Thus as $b-a$ decreases the charge transfer shown in Diagram 7 from planes to chains decreases. The calculated changes in electron transfer are quite small, in keeping with the rather small geometrical changes involved.

Figure 13 shows how the charges on the various copper atoms change with the geometry of the system. Two distortions are shown which couple the observed structure to an idealized one where all bond angles are either 90° or 180°, and all Cu-O distances are equal. As the Cu-O distances around Cu(1) shorten in the z direction so the z^2-y^2 band is pushed up in energy and electrons move to the planes, and as the $Cu(2)O_2$ planes are puckered the x^2-y^2 bands of the planes drop to lower energy and more electrons move to Cu(2). The result (see the calculated charges) is that the oxidation state of Cu(1) is higher than that of Cu(2), which is what we expect from the structural chemistry described in Sec. II. However, after these two distortions there is still overlap between the x^2-y^2 bands of the planes and the z^2-y^2 band in the chains. These two geometrical changes are thus very important in determining the electronic picture here.

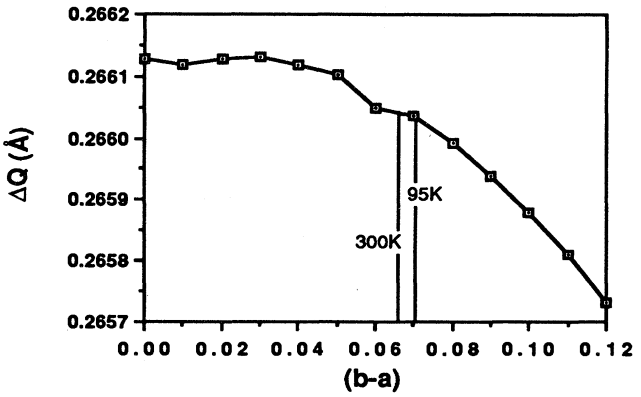

FIG. 12. Computed changes in the charge transfer from planes to chains with increasing $b-a$. Parameters appropriate for room temperature and 90 K are shown.

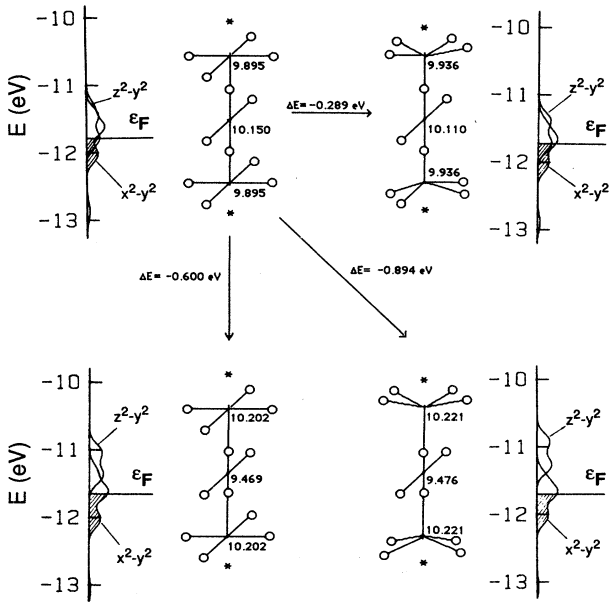

FIG. 13. Structural changes leading to the observed geometry for the 1:2:3 compound. Shown are the computed stabilization energies for each distortion and the electron densities at each center. Notice that the number of electrons computed for the square-planar chain (Cu^{III}) atoms is smaller than that for the plane (Cu^{II}) atoms.

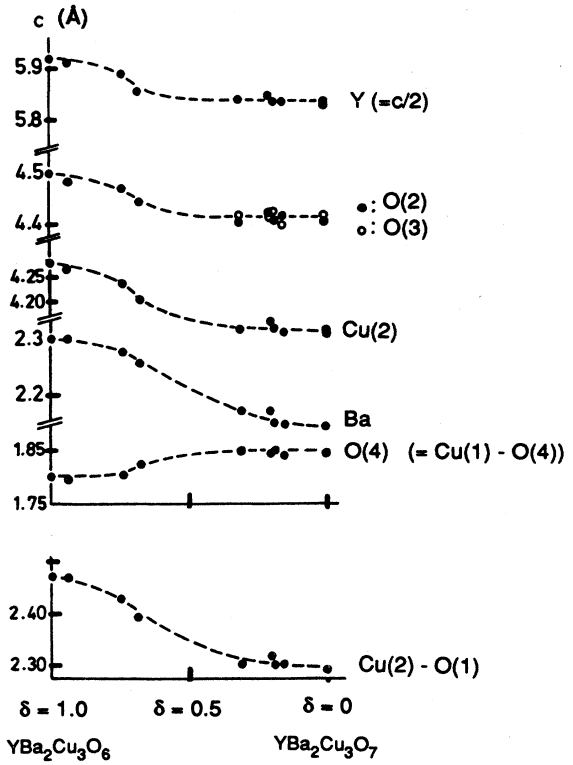

FIG. 14. Changes in geometry as a function of oxygen stoichiometry for the 1:2:3 compound. Shown are the changes in z coordinate for the relevant atoms.

It is now quite clear that the dependence of T_c on oxygen stoichiometry is crucially controlled by the oxygen ordering and we will study some of this below. There are several experimental observations which are of use to us here. Figure 14 shows from an earlier study[55] how the geometric parameters which describe the atomic positions in $YBa_2Cu_3O_{7-\delta}$ vary with δ. There are other more recent studies which emphasize this point.[52] These plots show the change in distance (along the x axis) of the various atoms in the structure from the plane formed by the Cu(1) atoms. These data come from high quality structural studies. The simplest explanation of these results is that the geometry changes are driven by the change in oxidation state of one-third of the copper atoms, associated with the coordination number change of chains to dumbbells, and the movement of the electropositive barium atoms in response to the presence of oxygen vacancies. It is the shape of these curves which are particularly interesting, as we have pointed out before.[55] The dependence of the structural parameters on x is not the linear one, expected on the basis of Végard's law. In fact there seem to be two relatively flat regions, $0.69 < \delta < 1$ and $0 < \delta < 0.31$, connected by a curve with a much steeper slope. Such behavior is typical of the behavior of two-phase systems, where the parametric dependence on composition is determined by attractive like-with-like interactions.

Thus from these data we may conclude that the defects are not ordered randomly for $\delta > 0$, but are organized so as to produce regions of Cu^{III} atoms separated from regions of Cu^{I} atoms. Such a conclusion is in accord with electron diffraction studies,[56] which show that the oxygen vacancies are indeed locally ordered. X-ray absorption studies also show Cu^{I} in oxygen defective samples of the 1:2:3 compound supporting a similar viewpoint.[57,58] From such a simple model the steeper slope at high δ (larger fraction of Cu^{I}) compared to that at low δ (larger fraction of Cu^{III}) implies that the clustering energy for Cu^{III} is stronger than that for Cu^{I}. There is thus nothing special on this model about the oxygen 6.5 stoichiometry, the one which gives an average copper oxidation state of II. As oxygen is removed from the compound $YBa_2Cu_3O_7$ the Cu-O distance remains little changed until $\delta \approx 0.6$. Associated with this sudden change appears to be the movement of T_c to zero (Diagram 1).[52] An important feature of the geometry is that at around this stoichiometry the Cu(1)-O(4) distance shrinks from ~ 1.85 to ~ 1.80 Å. Our calculations for this geometry show that there is now no charge transfer of electrons from planes to chains for this case, and thus the x^2-y^2 bands of Cu(2) can become close to half-full with the associated set of electronic factors which work against metallic behavior. The important result from our study is that it is because of this shortening of the Cu(1)-O(4) dis-

tance that the z^2-y^2 band is pushed to much higher energy and is not now able to remove electron density from the planes, shown schematically in Diagram 8.

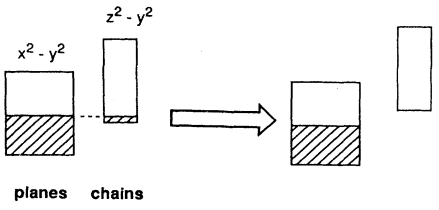

8

There is a change too in the degree of puckering of the $Cu(2)O_2$ planes which will lead to a raising in energy of the x^2-y^2 bands but we find that it is the former motion which wins out in controlling the $(z^2\text{-}y^2)/(x^2\text{-}y^2)$ separation. The chemical model then allows one to see how the geometry changes lead in a quite well-defined way to the controlling of the actual electron density in the x^2-y^2 band. We stress here, however, that our values for the electron transfer density are illustrative only, even though they come from our numerical calculations. Methods better than ours will be needed to get this right. We study the details of the oxygen vacancy ordering below.

bital drops in energy. This is shown schematically in Diagram 9.

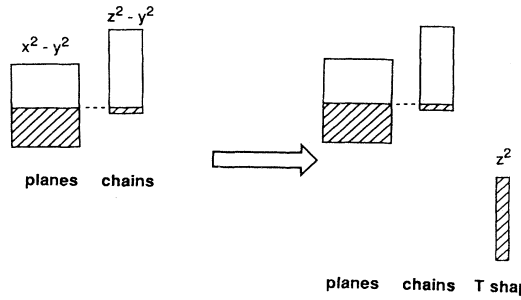

9

It is how the electrons are distributed among these bands that is important.

Consider first a unit cell doubled along b. If one O(1) atoms is lost from this cell (case A, Diagram 10)

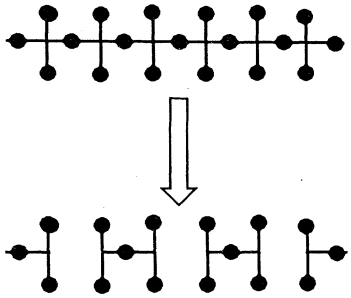

10

Vacancies

As we[59] and others[60] have pointed out, treating the defects in a rigid band sense by adding 2δ electrons to the Fermi level of the structure calculated with $\delta=0$ is a poor approximation. Here we build on our earlier ideas and generate some rules for the evaluation of the Fermi level for defect structures. As we have noted for $\delta>0$, it is the oxygen atoms associated with the copper atoms in the chain which are removed. By performing tight-binding calculations on periodic defect structures we can study the effects of various types of oxygen defects on the electronic structure. Our results are generally applicable to both the 1:2:3 and 2:1:4 systems and probably also to the 2:2:1:3 system. This approach implies that each defect structure should be regarded as a new structural type rather than as a minor perturbation of the parent. Four distinct cases are considered. In some cases the Fermi energy and/or the density of states at the Fermi energy $N(\varepsilon_F)$ changes appreciably due to shifts in position of the orbitals as a direct result of the changes in the local geometry. Experimentally,[61,62] for $YBa_2Cu_3O_{7-\delta}$ the majority opinion is that it is the O(1) atoms connecting square-planar metal atoms which are the ones most readily removed. (There is one recent study[63] that claims that it is the O(4) sites which are defective.) There are several ways in which this may occur. However this happens, the coordination number of some of the copper chain atoms is lowered and (see Fig. 2) the highest-energy d orbital drops in energy. This is shown schematically in Diagram 9.

then each of the copper atoms associated with the defect (two of them) will lie in a T-shaped environment. We can use the results of Fig. 2 to understand the results from the computed band structure. Figure 15 shows the orbital composition of the computed densities of states for the parent with $\delta=0$, and a periodic solid of stoichiometry $YBa_2Cu_3O_{6.5}$ for this case. The two z^2-y^2 orbitals, and hence bands associated with these coordination geometries, drop to lower energy and below the Fermi

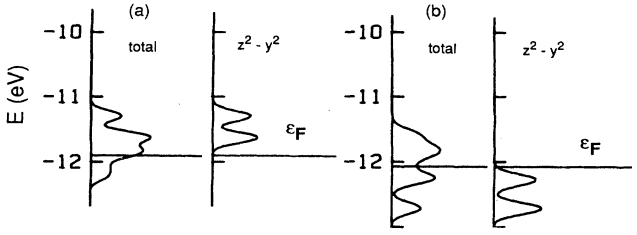

FIG. 15. Computed total and partial densities of states for (a) the parent structure $YBa_2Cu_3O_7$ and (b) a defect structure of stoichiometry $YBa_2Cu_3O_{6.5}$, where the oxygen vacancies of the periodic solid are arranged as described for case A. In (a) the partial density of states associated with the z^2-y^2 band of the chain is shown, and in (b) it is the contribution from the analogous band of the copper atom associated with the defect.

energy of the parent Diagram 9. However, only two extra electrons are present to fill them since a single oxygen atom has been removed. Thus, loss of an oxygen atom in this way will result in depression of the Fermi level, since electrons are removed from the highest occupied levels of the Cu^{II} atoms to fill these orbitals. The computed values of the Fermi level are -12.079 and -11.904 eV for case A and the parent, respectively. There is also a drop in the Fermi energy density of states $N(\varepsilon_F)$ to about half the value found for the parent. This also shows up dramatically in the plots of Fig. 15. A second pattern (case B, Diagram 11)

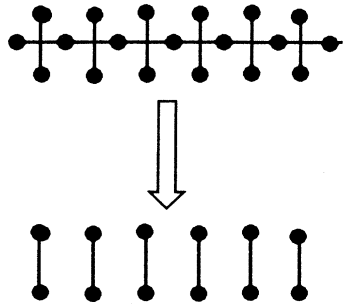

11

may be identified with a cell doubled along a with loss of an oxygen atom in such a way so as to give an equal mixture of square planar (Cu^{III}) and linear two coordination (Cu^{I}) in chains which alternate in character along a. This results in no change in Fermi-level location (calculated to be -11.904 eV) since now only one atom per doubled unit cell contains a deep-lying z^2-y^2 orbital (the two-coordinate geometry) with two electrons to fill it. Here we calculate virtually no change in $N(\varepsilon_F)$. We find case B with its linear, rather than T-shaped, Cu^{I} atoms to be the more attractive from a chemical point of view. Chemists generally do not associate the T-shaped structure with Cu^{I}, which is the natural result of the generation of oxygen defects. We have suggested[55] that a part of the driving force for ordering is the minimization of the number of such geometries. Raveau[42] has referred to such a geometry as an "abnormal" one for Cu^{I}.

These ideas then suggest that the real situation is much more complex than that implied by a rigid-band model, and that the location of the Fermi level is very much controlled by the way the defects are ordered via the geometrical structure of the solid. It is of course much more difficult (and presently is not possible) to calculate the energy associated with the defect, and thus explore the energetics associated with the various patterns. The whole question of the computation of bond energies is fraught with difficulty, since electron correlation plays an important role here. To be able to accurately get a measure of the energetics of the problem we need to be able to accurately calculate the energies of two-, three-, four-, and five-coordinate copper atoms. Our philosophy, therefore, has to be one in which we compare the energies of structures where the coordination numbers are as similar as possible.

There are other sites that in principle may be associated with the defects, namely the basal sites of the square pyramids. The picture that results is very similar for both the $YBa_2Cu_3O_{7-\delta}$ and $(La,Sr)_2CuO_{4-\delta}$ systems. Removal of a single oxygen atom [O(2) or O(3)] in a $YBa_2Cu_3O_7$ cell (case C) will result in a marked drop of the half-full x^2-y^2 orbitals associated with the two atoms to which the oxygen is coordinated since the result is a T-shaped geometry at two copper atoms. With deeper lying, and now doubly filled, x^2-y^2 and z^2 orbitals there is no change in the Fermi level of the material (we calculate -11.095 eV) as long as the geometry is not relaxed. Two half-filled orbitals drop below the Fermi level and two extra electrons from the missing oxygen atom fill them completely. As a result two Cu^{II} atoms have now become Cu^{I}. Removal of every O(2) or O(3) atom along either a or b, respectively, in one of the CuO_2 sheets (case D) leads to a chain of two-coordinate copper atoms. Since the x^2-y^2 orbital associated with it drops in energy (Fig. 2), and is now doubly filled, an extra electron must be added at the Fermi level. The result predicted using this approach is half as large as expected on the rigid-band model. The Fermi level is computed to lie at -11.787 eV for this case. As we have mentioned this result is in principle directly applicable to $(La,Sr)_2CuO_{4-\delta}$, but here the present view is that there are no oxygen defects for low strontium doping levels.

Change in planar charge density with oxygen stoichiometry

In this section we will tie together many of the geometrical-electronic relationships described above to make some suggestions as to how the number of electrons in the x^2-y^2 band of the Cu(2) atoms varies with oxygen stoichiometry, i.e., δ in $YBa_2Cu_3O_{7-\delta}$ (where $0 \leq \delta \leq 1$). Although the connection is at present tenuous we will show a correlation between this parameter and the observed behavior of T_c. (Certainly though, suppression of the electronic and geometrical instabilities associated with the diamagnetic half-filled band is strongly linked to charge transfer possibilities.) What we wish to explore is how the variation in Cu(2) electron density with oxygen stoichiometry is influenced by the geometrical effects we have mentioned above.

The sketching out of the charge density as a function of δ relies upon knowing the geometric details of the materials. Although there have been many structural studies, the fine details are unfortunately not as well established as we would like. The variation in cell parameters with δ is now well known, but the identity of the sites from which oxygen is lost is still not completely determined. Most studies show loss of oxygen from the planes perpendicular to z which contain the Cu(1) atoms. However, both O(1) and O(5) sites [see Fig. 4(a)] seem to be occupied for $\delta > 0$. We suspect that there are locally ordered regions of the structure so that such a result may be understood in terms of chains of square-planar copper atoms in chains of varying lengths running in both the a and b directions. One way of regarding the tetragonal structure is thus as an equal mixture of the two. There is some experimental evidence that supports this.[64] Some other studies show atoms missing from the O(4) sites.

Oxygen in these positions must eventually reappear with increasing δ, since they are fully occupied in the stable structure with $\delta=1$. We shall use here a model where oxygen is lost from the O(1) sites. Figure 16 shows in a schematic way how the band structure of the material changes with increasing δ. The number of levels (represented by the breadth of the box in the picture) associated with the x^2-y^2 bands of the planar copper (Cu^{II}) atoms remains constant, but loss of oxygen atoms from the chains generates Cu^{I} atoms at the expense of Cu^{III} atoms. The two-coordinate Cu^{I} atoms are represented by empty space, the Cu^{III} atoms by lines indicating chains.

As shown in the preceding section, loss of a single oxygen atom in a $Cu(1)O_3$ chain gives rise to a loss of electrons from the x^2-y^2 bands of the planar copper atoms, but an ordered collection of adjacent vacancies will lead to no loss of electrons from this band. As more oxygen is lost then the probability of forming clusters of vacancies naturally increases. At $\delta=1$ with perfect ordering there are of course no Cu^{III} z^2-y^2 levels (Fig. 16) and the x^2-y^2 bands of the planar copper atoms are exactly half-full. If our interpretation of the x-axis plots of Fig. 14 is correct, then ordering is occurring for low δ. The number of electrons removed from the x^2-y^2 bands of the planar copper atoms should then have the functional dependence on δ as shown with a dashed line in Diagram 12.

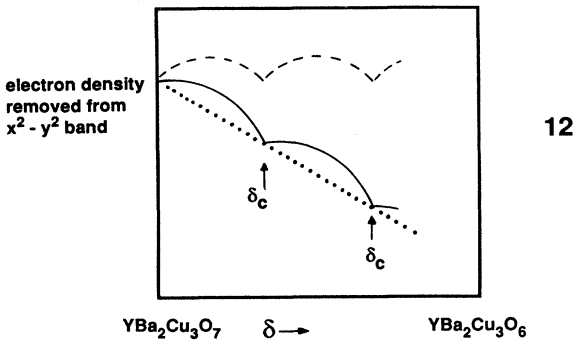

12

δ_c is some critical point where an ordered structure is found. (We have, not-so-arbitrarily, chosen this as multiples of a third; our reasoning becoming apparent below.) We know too that $b-a$ decreases with increasing δ. If this is interpreted literally, then as shown above, the z^2-y^2 band of the chain copper atoms is pushed to higher energy and electron transfer to the chains reduced (shown with a dotted line in Diagram 12). The combination of the two effects is an electron density plot (the solid line) that is roughly flat for low δ and then drops whenever there is a strong ordering of vacancies. There is already a correlation between T_c and the amount of Cu^{III} (interpreted here as square-planar copper atoms) measured experimentally,[53] which has steps similar to the one in Diagram 12.

At the point when the Cu(1)-O(4) distance suddenly shortens (the c-axis anomaly) then the electron transfer to the chains is abruptly cut off and the planar copper atoms have exactly half-filled x^2-y^2 bands. We can extend our plot of Diagram 12 with this result to give Diagram 13.

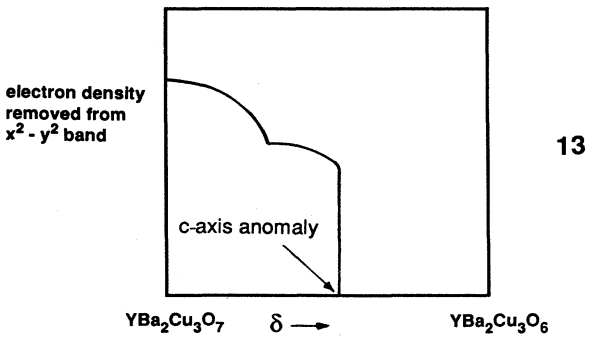

13

It is then tempting to compare the plot with that of Diagram 1. This approach does have the obvious flaw in that the observed variation in $b-a$ with δ might come about simply as a result of disorder in O(1) and O(5) sites rather than being intrinsically a function of Cu-Cu distance within the chains. However, we do note that the effect of removing electrons from the Fermi level by the introduction of isolated vacancies will also tend to reduce the density in the Cu^{III} z^2-y^2 band, resulting in a shortening of b

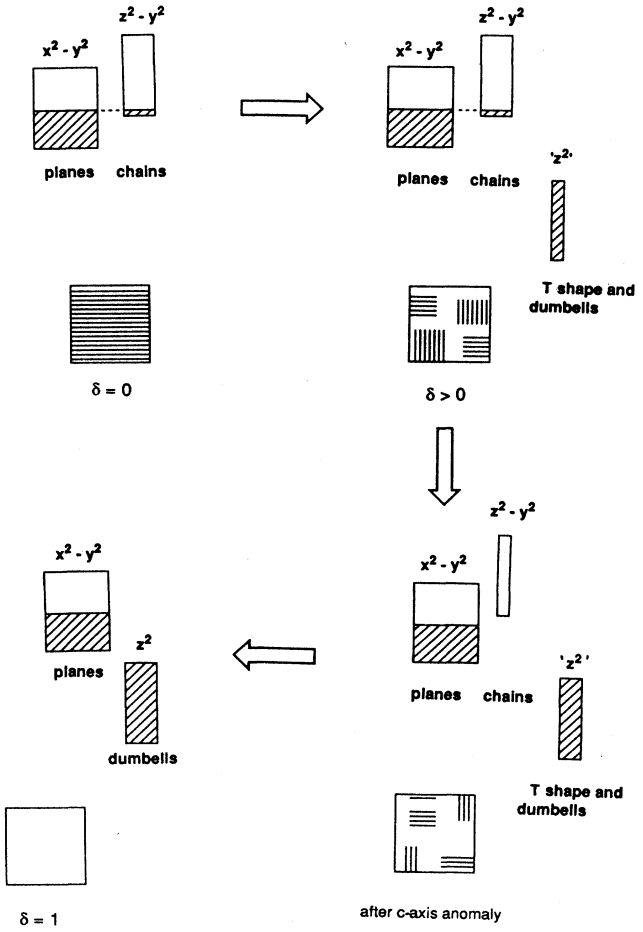

FIG. 16. Schematic band structure variation in the 1:2:3 compound with oxygen stoichiometry. At the bottom of each figure is a schematic picture showing the arrangement of regions of chain (Cu^{III}) atoms (lines) and dumbbell (Cu^{I}) atoms (space).

as a result of less population of Cu^{III}-O antibonding orbitals. Sorting out the competition between the two effects will be difficult. A conclusion of the approach is that an ordered structure of some type occurs at $\delta \sim 0.33$.

IV. STRUCTURAL ALTERNATIVES FOR 1:2:3

The logic of the observed structures of $YBa_2Cu_3O_{6,7}$ are now clear; they are consistent with the local geometries preferred by the various oxidation states of copper. Alternatively, the observed pattern of defects in the $AB_2C_3O_9$ perovskite structure (this has a trebled ABO_3 formula for comparison with the 1:2:3 structure) to give $YBa_2Cu_3O_7$ can be understood by the driving force associated with the Jahn-Teller instability of octahedral Cu^{II} or Cu^{III}, leading to, respectively, loss of one ligand or two trans ligands. It is interesting to devise other possible structures for the parent compound in order to shed more light on the reasons behind the stability of the observed arrangement. We will proceed in two steps. First we will devise some structural alternatives and examine their stability relative to the observed structure. Then we will take the most likely alternative of this set, examine its possible distortion modes, and ask how we may perhaps stabilize it by the insertion of suitable cations. The structural possibilities are of two types. In the first, although the overall stoichiometry is correct, the sum of the oxidation states at copper as indicated by the local coordination geometries is not consistent with the number of oxygen atoms. As a result it may be excluded on simple chemical grounds. In the second type there are no such problems of this type and we need to search further for more detailed electronic reasons. We are of course limited only by our ingenuity in inventing new structures, but here we discuss just three possibilities.

Figure 17 shows two structures (X, Y) that have the same triple copper layer structure of the observed $YBa_2Cu_3O_7$ arrangement, but with different arrangements of the oxygen vacancies between them. In all three structures the copper atoms in the plans are square-pyramidally coordinated by oxygen. The only difference lies in the ordering pattern of the oxygen atoms associated with the middle sheet of copper atoms, as shown in Fig. 17(d). Infinite chains of Cu-O linkages are a feature of the first two structures, but in the alternative there is some cross-linking which gives rise to octahedral coordination. A natural result is the generation of linear two-coordinate units. In the second, alternative slabs of the first are shifted by $a/2$. Table II lists the number of coordination geometries of each type that result. For both $YBa_2Cu_3O_6$ and $YBa_2Cu_3O_7$ the number of square pyramidal, linear, and square geometries are consistent with the oxygen stoichiometry. For alternative X, however, we would probably expect nine Cu^{II} (the octahedral and square-pyramidal units) plus one Cu^{I} (the linear unit) and two Cu^{III} (the square-planar units). This total is inconsistent with the number of O atoms counted as O^{-2}. For alternative Y with ten Cu^{II} (the square-pyramidal units) plus one Cu^{II} (the linear unit) and one Cu^{III} (the square-planar unit) the same comment applies. In both alternative structures we have shown (Fig. 17) equal Cu-

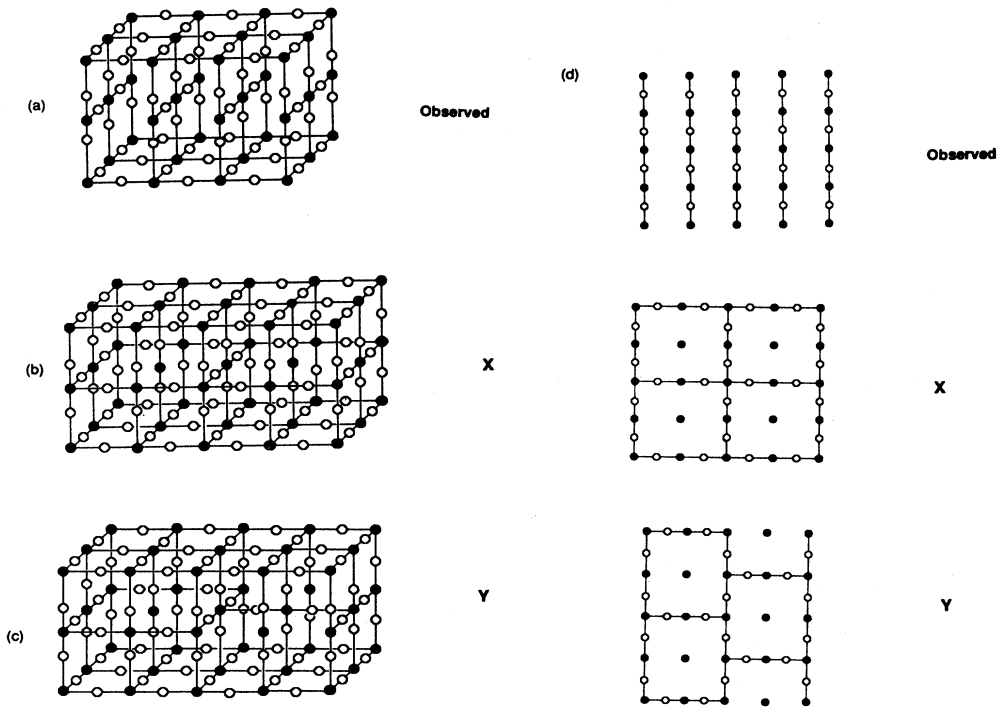

FIG. 17. Idealized descriptions of alternative structures for the 1:2:3 compound. (a) The observed structure, (b) variant X, (c) variant Y, and (d) atom ordering in the middle layer of the slab for observed, X, and Y variants.

TABLE II. Coordination geometries in structural alternatives.

Coordination geometry	Linear	Number of copper atoms with these coordination geometries[a] Square	Square pyramidal	Octahedral
Coordination number	2	4	5	6
Observed $YBa_2Cu_3O_7$	0	4	8	0
Observed $YBa_2Cu_3O_6$	4	0	8	0
Alternative (X) $YBa_2Cu_3O_7$	1	2	8	1
Alternative (Y) $YBa_2Cu_3O_7$	1	1	10	0

[a]The cell chosen if four times as large as the smallest unit cell for the observed $YBa_2Cu_3O_7$ structure.

O distances. In practice some variety is to be expected, since the oxygen atoms are attached to copper in different oxidation states. Relaxation of those idealized structures to take care of this problem, however, will be difficult to accomplish given the connectivity of the lattice. Some energetically unfavorable strain will result.

A third structure Z, which contains the same set of structural elements found in the observed arrangement, is shown in Fig. 18 along with views of the observed structure. It is made up of square-planar units condensed into a sheet and pairs of head-to-head square pyramids also condensed into a sheet. It does not suffer from the electronic problems we have just mentioned for X and Y. Our calculations suggest that this presently unknown structure will not be as stable as the observed one, but only a little less stable, and such an energy difference may be compensated by more favorable ionic interactions which are not included in our computations. It is interesting, however, to try to understand the origin of this "covalent" energy difference. An obvious point is that the mutually apical oxygen atom linking the two sheets would be weakly bound to them, and thus readily lost.

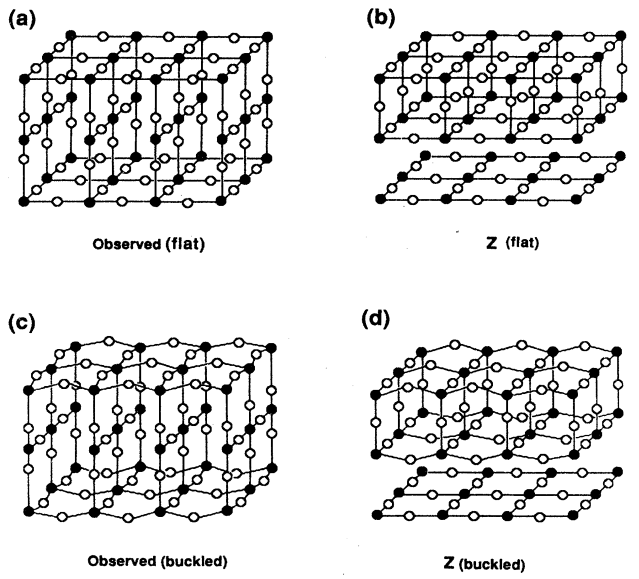

FIG. 18. A further alternative for the 1:2:3 compound, compared to the observed arrangement. (a) Idealized observed structure, (b) idealized variant Z, (c) observed structure with sheet puckering, and (d) relaxed variant Z.

This would give a material of stoichiometry $YBa_2Cu_3O_6$ containing square-planar copper atoms more appropriate for Cu^{III} or perhaps Cu^{II} than for $Cu^{I/II}$. Stable molecules, however, are known in which a ligand is sandwiched between two planar $Cu^{II}L_4$ units and attached by two long Cu—ligand bonds. $(Cu^{II}L_4)_2$ pyrazine is an example.[65] There will be structural elements of this type in oxygen-rich materials with stoichiometries $YBa_2Cu_3O_{7+x}$ ($x > 0$) if the extra oxygen atoms enter the Y layers.[6]

A second point to consider is how much structural flexibility there is which can allow the band structure and electron filling of the orbitals of the metal atoms in the isolated planes to be consistent with the oxidation states demanded by the geometry. For example, the alternative structure is tetragonal and the arrangement of the sheets is such that the Cu-O distances within the isolated sheet have to be identical to the distances within the slabs if the apical-basal angle is set at 90°. Since the x^2-y^2 bands are unaffected by coordination of atoms in the z direction (see Fig. 2) a schematic band structure (from the results of our numerical computations) would be that of the left-hand side of Diagram 14

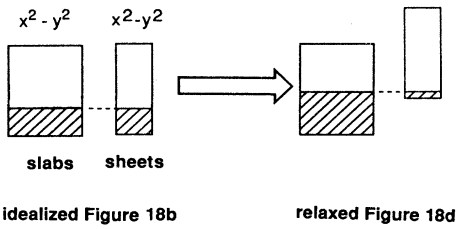

14

and show that the x^2-y^2 bands of each copper atom are equally populated. Thus, unlike the observed structure where the connectivity allows a Cu^{III} atom to behave as such, the idealized alternative structure does not. However, one simple way of overcoming this problem is to allow the five-coordinate copper-containing sheets to buckle as shown in Fig. 18. As a result these copper atoms are now more pyramidal and, if the a and b axes remain unchanged, are associated with longer Cu-O distances. Both the Cu—O bond length change and the change in

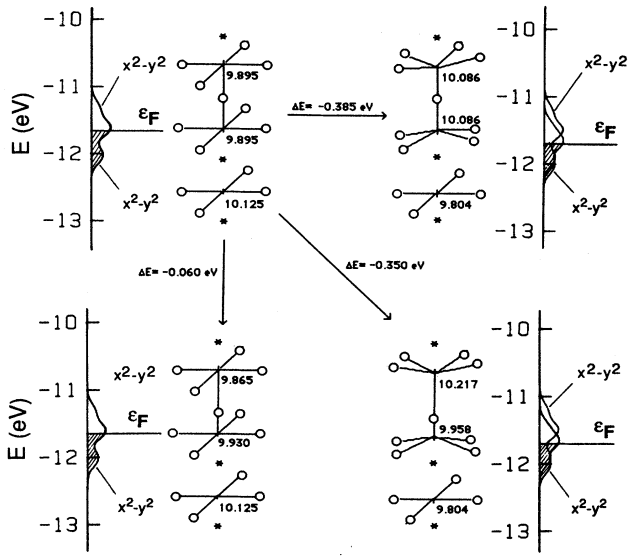

FIG. 19. Structural changes leading to the relaxed geometry for variant Z of the 1:2:3 compound. Shown are the computed stabilization energies for each distortion and the electron densities at each center. Notice that for the bent slab structures the number of electrons computed for the square-planar isolated sheet (Cu^{III}) atoms is smaller than that for the plane (Cu^{II}) atoms in the slab.

angle give rise to a drop in the mean position of the slab copper x^2-y^2 bands. Electron density is removed from the x^2-y^2 band of the isolated sheet, which now becomes more Cu^{III}-like, and donated to the x^2-y^2 band of the slab, which now becomes more Cu^{II}-like, Diagram 14. The numerical results of our calculations are shown in Fig. 19, a picture which merits comparison with Fig. 13. The two structures are thus very similar. In the alternative structure the $Cu^{III}O_2$ planes can play the same role as the $Cu^{III}O_3$ chains in the observed one. There is, however, in the alternative structure no distortion analogous to the shortening of the Cu(1)—O(4) bond in the observed structure. However, there is a soft motion which leads to asymmetry at the central atom of the slab. Such motions are common in perovskite materials,[66] and might be stabilized by a judicious choice of cation.

A third way to understand the energy of the new structure relative to the observed one is to investigate this difference as a function of d count. Figure 20 shows such an energy-difference curve using idealized (equal Cu-O distances and 90° angles) for the pair of structures. Notice that for $d^{8.67}$, the average number of d electrons per unit cell calculated from the stoichiometry, the observed structure is found to be more stable. Such plots may usefully be interpreted using the method of moments.[46–48] Briefly, if the electronic densities of states of two structural alternatives differ at the mth moment, then the energy-difference curve between them as a function of band filling x will have m nodes, counting the two at the full ($x=1$) and empty ($x=0$) points. Such an approach has been shown to be useful in understanding[31] the defect ordering pattern in the material $CaMnO_{2.5}$. The method relies upon the important connection between the nth moment of the electronic density of states and the weighted sum of all the self-returning walks of the orbital network of length n. The weight of a given walk is the product of all the H_{ij} integrals involved in the interorbital walks. In practice all we need to do is find out the first set of walks which are different between the two structures, and this immediately gives us the form of the energy-difference curve. For our present series of compounds the σ- and π-bonding manifolds are full at d^0, and so this point corresponds to $x_\pi=0.5$ and $x_\sigma=0.5$. d^{10} corresponds to $x_\pi=1$ and $x_\sigma=1$. The two types of interactions give rise to orthogonal levels (if the O—Cu—O bond angles are set, as they are in these calculations, at either 90° or 180°), but the σ and π bands overlap as shown in Diagram 15.

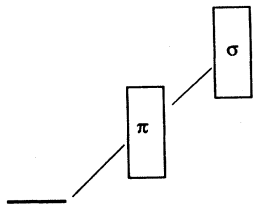

15

In Fig. 20 there are two parts to the energy-difference curve, of similar shape but of different amplitudes as shown in Diagram 16.

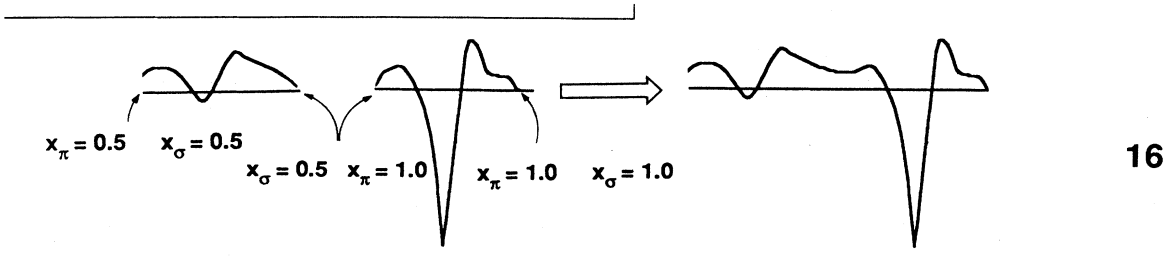

16

One is largely controlled by the π-type interactions (d^0 to approximately d^6) and the other by the more energetic type σ interactions (approximately d^6 to d^{10}). At around d^6 the pair of oscillations overlap. Each part of the electronic problem is thus apparently a sixth moment one since there are three nodes between $x_{\sigma,\pi}=0.5$ and $x_{\sigma,\pi}=1$. The origin of this result is easy to see from Diagram 17.

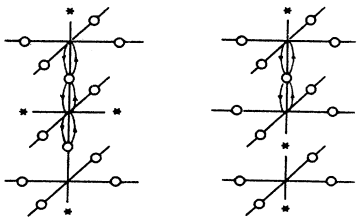

17

The two structures first differ at the sixth moment, since it is a walk of this length that allows a square-pyramidal copper atom in the alternative structure to "see" the vacancy (marked with an asterisk) in the structure along c. The observed structure has the larger number of six-walks, and from the methodology of the moments method[46–48] will be the more stable structure at $x_{\sigma,\pi}=0.5$ as calculated.

Our results suggest that overall the observed structure should be more stable, but the energy difference between the two alternatives is not large at the relevant electron count. How might we stabilize this new geometry?

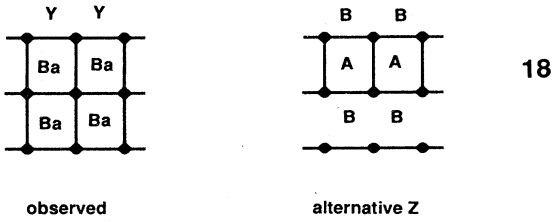

18

Diagram 18 shows one observation which may be important, namely the sizes and types of counterion in the structure. In the observed structure there is one Y^{3+} ion between the slabs and two Ba^{2+} ions within a slab. In the alternative structure there will be one A ion within the slab and two B ions separating slabs and sheets. To maintain charge balance the alternative can either be written $A^{+}(B^{3+})_2Cu_3O_7$ or $A^{3+}(B^{2+})_2Cu_3O_7$. Given the dimensions of the observed structure we seek A^{+} ions which are similar in size[67] to Ba^{2+}, and B^{3+} ions which are similar in size to Y^{3+} for the former arrangement (potassium and yttrium are perhaps the obvious pair), and A^{3+} ions which are similar in size to Ba^{2+} and B^{2+} ions, which are similar in size to Y^{3+} for the latter arrangement. Ag^{2+} and Cd^{2+} are of similar size to Y^{3+}, but it is difficult to find a trivalent ion as large as Ba^{2+}. Bi^{3+}, Ce^{3+}, and La^{3+} are the largest but somewhat smaller. $KY_2Cu_3O_7$ and $AgLa_2Cu_2O_7$ might be possible synthetic goals. However, for the latter one might prefer to substitute silver for the copper in the structure rather than fill the voids within the copper oxide framework.

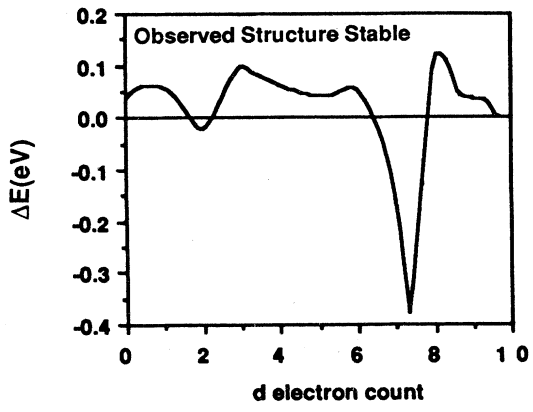

FIG. 20. Computed variation in the energy difference between the idealized 1:2:3 compound and variant Z as a function of d electron count.

V. THE 1:2:4 COMPOUND $YBa_2Cu_4O_8$

Electronic structure

This is a particularly interesting system[68] since at the stoichiometric composition it has to contain copper in nonintegral oxidation states. We will see that a striking feature of the electronic structure is how the geometry of the system naturally allows such a process to happen. This material (Fig. 21) contains the simple pair of CuO_2 sheets that are present in the 1:2:3 compound, but instead of single vertex-sharing CuO_3 chains between them, it contains edge-sharing CuO_2 double chains. An obvious way to write the chemical formula, if we insist that the pair of infinite CuO_2 sheets contain Cu^{II}, is as $Y^{III}Ba^{II}_2(Cu^{II}O_2)_2(Cu^{II/III}O_2)_2$. An examination of the band structure of the material shows how this comes about. Recall that in the 1:2:3 compound the z^2-y^2 band lines at higher energy than the x^2-y^2 bands, as a direct result of the shorter Cu-O distances within the chains compared to those in the planes. Recall too that the two x^2-y^2 bands are only slightly split apart in energy as a result of their poor coupling through the chain orbitals. In the 1:2:4 compound, however, the width of the z^2-y^2 band of the double chains is considerably larger than that found for the same orbital of the single chains in the 1:2:3 compound, since now the interaction between the two z^2-y^2 orbitals per cell is large, coupled through adjacent oxygen orbitals. Figure 22 shows the computed densities of states for the system, and indicates now a much larger overlap between chain orbitals and plane orbitals than

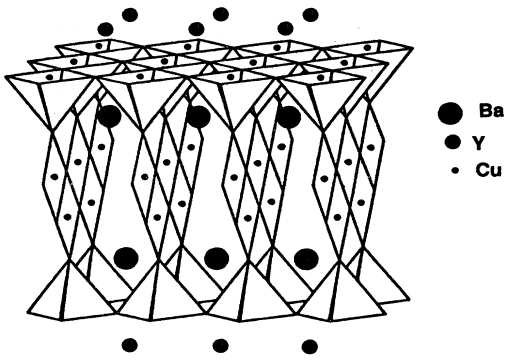

FIG. 21. The observed structure of the 1:2:4 compound $Y^{III}Ba^{II}_2(Cu^{II}O_2)_2(Cu^{II/III}O_2)_2$.

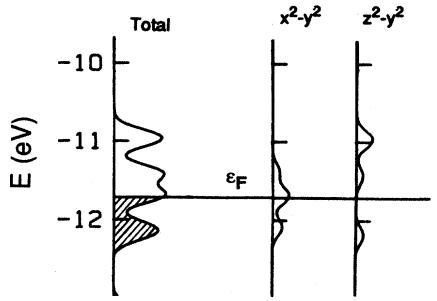

FIG. 22. Computed density of states for the highest occupied bands of the observed 1:2:4 compound. Shown is the total density of states and the partial densities for the x^2-y^2 orbitals of the planes and the z^2-y^2 orbitals of the double chains.

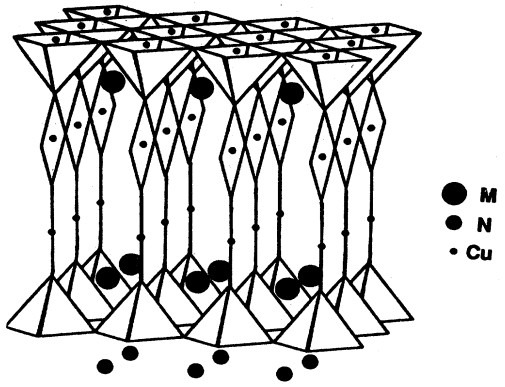

FIG. 23. The structural of an alternative for the 1:2:4 compound, which may be written as $Y^{III}Ba_2^{II}(Cu^{II/III}O_2)_2(Cu^{III}O_3)(Cu^{I}O)$.

was the case in the 1:2:3 compound. As a result there is extensive occupation of chain z^2-y^2 orbitals in this system and the oxidation state of the chain copper atoms will lie somewhere between two and three. Our computed charges are shown in Diagram 19(a).

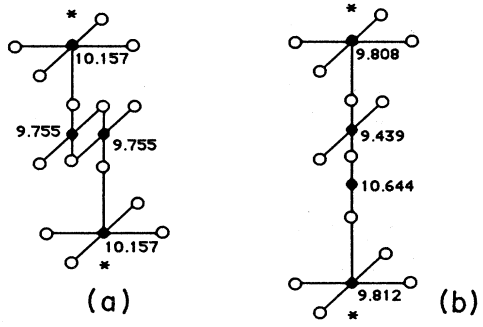

19

We should be careful in interpreting them literally, but a comparison between Diagram 19(a) and Figs. 13 and 19 shows that the description of the chain copper atoms as $Cu^{II/III})_2$ is not a bad one. The actual extent of electron transfer from planes to double chains to remove the half-filled x^2-y^2 band for Cu^{II} is as difficult to calculate using our approach as it was for the 1:2:3 compound. (T_c here is[68] 80 K).

Structural alternative

At this stage we can ask why the obvious structural alternative of Fig. 23 is not found. Here the double chains of the observed 1:2:4 compound are replaced by a single chain linked to a dumbbell. The alternative thus contains features of the two 1:2:3 compounds with O_6 and O_7 stoichiometries. In terms of likely coordination geometries for the different oxidation states of copper we would write it as $Y^{III}Ba^{II}{}_2(Cu^{II/III}O_2)_2(Cu^{III}O_2)(Cu^{I}O_2)$ or $Y^{III}Ba^{II}{}_2(Cu^{II/III}O_2)_2(Cu^{III}O_3)(Cu^{I}O)$, depending on the (arbitrary) way we assigned the central oxygen of the intersheet unit. Figure 24 shows a calculated density of states for such a system which nicely reflects this assignment of oxidation states. The chain z^2-y^2 orbitals are empty (i.e., Cu^{III}), the dumbell z^2 orbitals are doubly occupied (i.e., Cu^{I}) and the sheet x^2-y^2 orbitals are certainly less than half full (i.e., $Cu^{II/III}$). The charges we compute for this arrangement are shown in Diagram 19(b) and support such an assignment by comparison with Figs. 13 and 19 and Diagram 19(a). We calculate from our band-structure computation a stabilization energy of 1.1 eV relative to that of the observed geometry. There are several uncertainties in this figure. First, the internuclear distances used in the calculation are the same as those found in the observed structure. Using our method we are not able to accurately model the energetics of bond length changes. Second, the influence of many-body terms here may be important too. As we have noted earlier, there is a large energetic penalty for the generation of Cu^{I} and Cu^{III} from Cu^{II}.

VI. THE 2:1:4 COMPOUND $L_{2-x}Sr_xCuO_4$

The orthorhombic-to-tetragonal transition

In contrast to the 1:2:3 compound where the relationship between the orthorhombic and tetragonal structures is associated with the ordering of oxygen vacancies, the

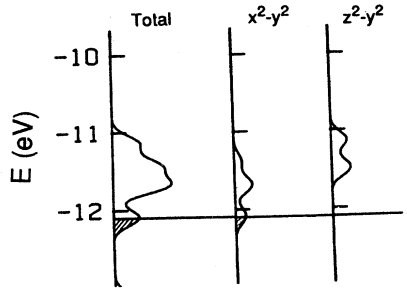

FIG. 24. Computed density of states for the highest occupied bands of the alternative 1:2:4 compound. Shown is the total density of states and the partial densities for the x^2-y^2 orbitals of the planes and the z^2-y^2 orbitals of the chains. Not shown is the deeper-lying full z^2 orbital of the two-coordinate dumbbells. Notice the clearly less-than-half-full x^2-y^2 band.

orthorhombic and tetragonal structures for the 2:1:4 ($La_{2-x}Sr_xCuO_4$) compound have the same atomic connectivity and copper and oxygen stoichiometry (Diagram 20).

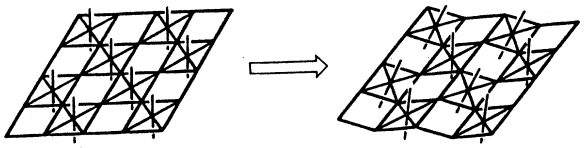

20

The current view is that there are no oxygen vacancies up to $x=0.2$. The orthorhombic structure (distorted with $a \neq b$) is a puckered version of the tetragonal form. In contrast to x-ray-absorption studies of the 1:2:3 compound, no Cu^I is found[57,58] as x increases from zero in similar studies on this material. Thus the effect of doping is to gradually remove electron density from the x^2-y^2 band of the system. We know that as the amount of strontium doping (x) increases (i.e., as the average copper d count decreases) the tetragonal structure gradually becomes more stable than the orthorhombic one. This manifests itself in a drop in the transition temperature for the transformation as x increases.[69,70] For example, with $x=0$ the orthorhombic-to-tetragonal transition occurs at 533 °C, with $x=0.15$ it appears at 190 °C, and with $x=0.2$ it is the only arrangement known. Figure 25 shows a calculated energy difference curve for the two structures as a function of d count using the $b-a$ value for the structure with $x=0$. Interestingly, it shows that the two structures are close in energy for d^9 but that as x increases, i.e., for $d<9$ the tetragonal version becomes more stable in accord with experiment.[70]

The electronic reasoning behind this structural transformation is similar to that described earlier for the 1:2:3 compound and is associated with the relief of antibonding Cu-O interactions by puckering as shown in Diagram 4. There, as the antibonding orbital becomes less full of electrons the puckering becomes less favored. Here the distortion to the orthorhombic structure becomes less favored as the doping level increases. Notice the maximal slope in Fig. 25 at electron counts corresponding to the electronic situation where σ antibonding orbitals are occupied. We may appreciate the difference in the response of the two systems to such an electronic state of affairs simply in terms of geometry. In the 1:2:3 compound the planar copper atoms are five-coordinate with the long Cu(2)—O(4) bonds on the same side of the plane. Simple puckering is an obvious geometrical route. In the 2:1:4 compound there are oxygen atoms on both sides of the plane, and thus bending at both oxygen and copper is achieved by a more complex route to relieve the instability of Diagram 4. If it is the occupation of antibonding orbitals which stabilize the distorted (orthorhombic) structure, what is the force behind the stability of the tetragonal one? From Fig. 25 it can be seen that this is the structure favored for the d^6 configuration and is also the geometrical arrangement we find to be favored for an oxide lattice where there are no metal atoms at all. Very often we find that in the absence of an electronic driving force, such as that of Diagram 4, associated with the occupation of antibonding orbitals, it is the "more symmetric" structure in terms of equality of internuclear separations which is the more stable. Behind such a result in the system described here is the importance of repulsions between the formally nonbonded oxygen atoms which can get quite close in the structure as a result of the short Cu-O distances. Thus the energetics of the tetragonal-to-orthorhombic distortion are a balance of directly bonded (Cu-O) and nonbonded (O-O) interactions. "Molecular mechanics" calculations[71] using pairwise potentials between the atoms in the structure have also been used to mimic this distortion. This result is not new in oxide chemistry. In our studies[72] on transition-metal oxides with the rutile (TiO_2) structure we found that the distortion of the idealized structure to the observed one was controlled by a similar balance. [Our calculations are not

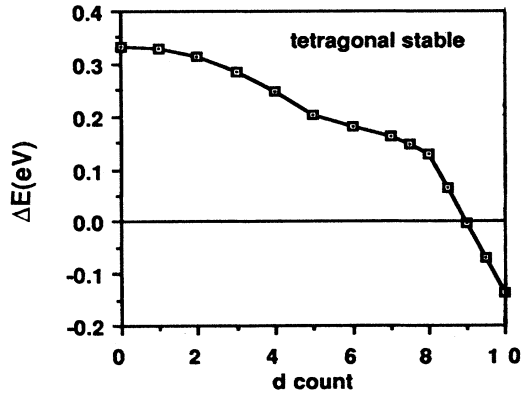

FIG. 25. Computed energy-difference curve between the tetragonal and orthorhombic forms of the 2:1:4 compound ($La_{2-x}Sr_xCuO_4$) as a function of electron count. In this calculation the value of $b-a$ chosen was that corresponding to $x=0.15$.

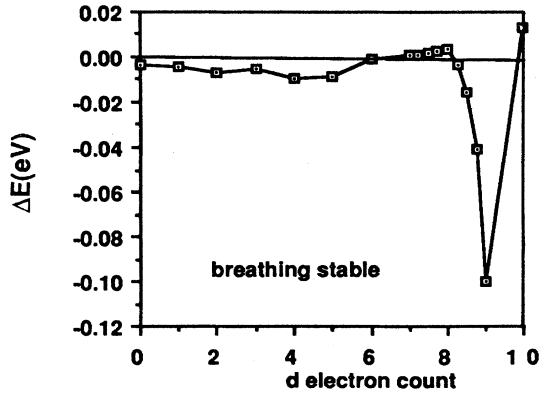

FIG. 26. Computed stabilization energy of the breathing mode [Diagram 5(a)] in the 2:1:4 compound as a function of the average number of d electrons per copper.

perfect in getting the balance between these two effects correct. If a value of $b-a$ appropriate for $x=0.15$ is used, the slope of the energy difference plot with d count is of opposite sign suggesting an underestimate of the O-O terms at this geometry.)

The tetragonal-to-orthorhombic transition is thus driven by simple relief of antibonding interactions and does not arise via a Peierls type of electronic situation. Of the volume conserving distortions of the tetragonal structure (a) shown in Diagram 21,

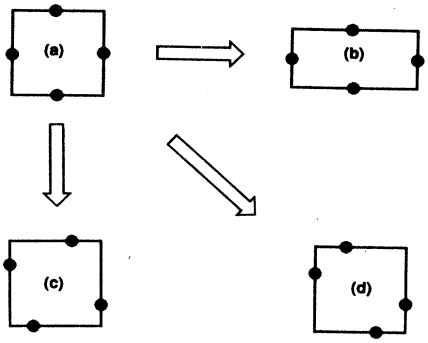

21

only (d) opens a gap at the Fermi level. Those giving (b) and (c) involve small energy changes. The distortion of Diagram 21(d) is the analog of the "breathing" motion described earlier for the 1:2:3 compound, and the energy difference curve (Fig. 26) is very similar indeed. It has the characteristic fourth-moment appearance described earlier and one which we associate with Peierls-type instabilities. A curve of this shape is not seen in Fig. 25. Similar comments to those made above concerning the breathing distortion in the 1:2:3 compound apply here as well.

The depletion of the x^2-y^2 band on the strontium doping, antibonding between copper and oxygen, shows up in the experimentally determined Cu-O distances. They become shorter, just as expected, as x increases [1.9035(1) for $x=0$ and 1.8896(1) for $x=0.15$].[69,73] There is a suggestion[11,12] that superconductivity depends upon the "covalency" of the Cu—O bond, measured via the Cu-O distance. As the covalency increases (i.e., as the Cu-O distance decreases) then superconductivity appears. The thrust of the arguments in this paper provide a different perspective. Thus, although as the Cu-O distance decreases, the bandwidths should increase and encourage the formation of a metallic state, the change in Cu-O distance may just be a reflection of how far away from half-filling is the x^2-y^2 band.

VII. THE 2:2:1:3 SYSTEM $Pb_2Sr_2(R_{1-y}M_y^{II})Cu_3O_{8+y}$ AND OTHER SYSTEMS

The newly discovered 2:2:1:3 system[74] $Pb_2Sr_2(R_{1-y}M_y^{II})Cu_3O_{8+x}$ (where R is a lanthanide or early three-valent transition metal such as yttrium and M^{II} is a two-valent ion such as Sr or Ca) has geometric-electronic features of both the 1:2:3 and 2:1:4 compounds

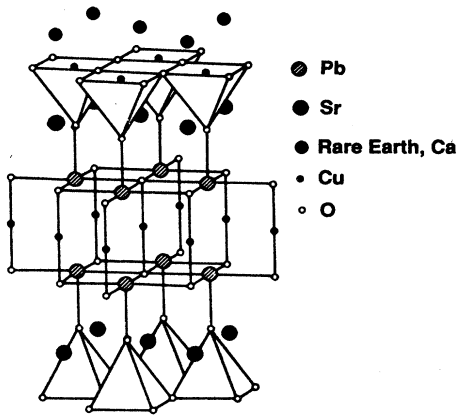

FIG. 27. The observed structure of the 2:2:1:3 compound $Pb_2Sr_2(R_{1-y}M_y^{II})Cu_3O_{8+x}$.

as we will see. It contains (Fig. 27) sheets of linked, square-pyramidal CuO_5 units (we will call these $Cu^{II}O_3$) and dumbell $Cu^{I}O_2$ moeties. These oxidation states fit well with the charge balance in the stoichiometric compound where $x=y=0$, namely $Pb_2^{II}Sr_2^{II}R^{III}/(Cu^{II}O_3)_2Cu^{I}O_2$. Such a description also comes from a band-structure calculation on the species.

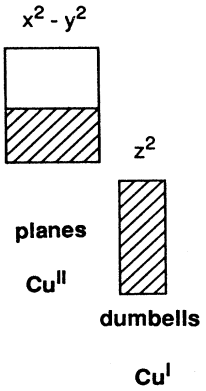

22

Diagram 22 shows a schematic picture extracted from our numerical computations using the orbital ideas we have developed earlier. When $y\neq 0$ but $x=0$, the electrons are removed from the x^2-y^2 bands of the Cu^{II} in much the same way as in the 2:1:4 compound and the electron occupancy moves off half-filling.

The behavior of the compound as x increases from 0 is interesting. Experimentally it is found that increasing the oxygen concentration (around $x=1.7$ is the highest achieved) eventually destroys the superconductivity behavior. Although it appears at first sight to be the converse of the result for the 1:2:3 compound, where superconductivity disappears from the O_7 stoichiometry as oxygen is *removed*, in electronic terms the two represent very similar situations if we assume that the first oxygen atoms are added to the region occupied by the $Cu^{I}O_2$ dumbells. These regions may be converted into chains of

square-planar copper atoms if $x = 1$. For x close to 0, T-shape CuO_3 units are formed (Diagram 23),

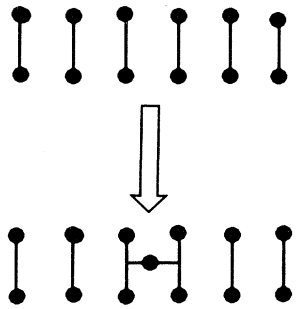

23

which we can clearly see is the reverse of the process for the 1:2:3 compound in Diagram 10. Since the z^2-y^2 band of such a unit lies below that of the x^2-y^2 bands of the Cu^{II}, two electrons have to be removed from the Fermi level to create a filled O^{2-} level. Thus initially, electrons are removed from the x^2-y^2 bands of Cu^{II} in excess of those removed by increasing y. By analogy with the 2:1:4 compound ($La_{2-x}Sr_xCuO_4$), where superconductivity disappears if x rises much above 0.15, it may disappear in the 1:2:4 compound for smallish x. However, the electronic situation is very different if the oxygen atoms order around the dumbells as described earlier for the 1:2:3 compound. Now square-planar units are created, Diagram 24,

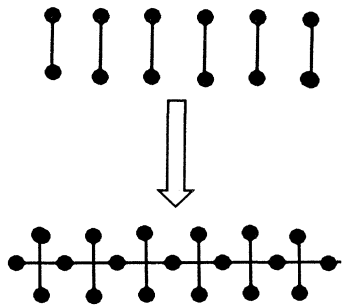

24

(this is just the reverse of Diagram 11) with the concimmitant generation of a z^2-y^2 band that may lie above the x^2-y^2 bands of the Cu^{II} planes just as in the 1:2:3 compound (Diagram 25).

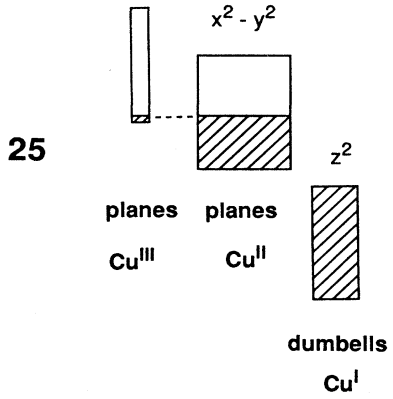

25

Recalling our discussion concerning the vacancies in the 1:2:3 compound, this situation will result in no change in the Fermi level. Two electrons are transfered from Cu^I to oxygen to give O^{-2} and Cu^{III}, and the z^2-y^2 band associated with these atoms is emptied (or close to it). Thus for high oxygen concentrations this model implies that the electronic situation will be very similar to that in the 1:2:3 compound with a high oxygen concentration. A superconductor could result. It will be very interesing to see if there are indeed two superconducting regions in this material as suggested by this model. The first should occur (and is seen) at low x, where removal of density from the half-full situation occurs via a combination of doping and adding oxygen and the other at higher x (~ 1), where charge transfer to Cu^{III} planes should be important. Thus the situation in $Pb_2Sr_2(R_{1-y}M_y^{II})Cu_3O_{8+x}$ is a very interesting one, containing features of the two systems we discussed earlier.

What about other systems? In this article we have focused on the geometrical and electronic structure of three copper-containing superconductors. We have not mentioned the bismuth and thallium containing copper oxide systems[75,76] for the simple reason that the geometrical details of these species are as yet not accurately known. One of the striking aspects of our discussion in this paper is surely the demonstration of the crucial control of the *electronic* structure by the *geometric* structure. We reserve comment until the details of the structures have been more accurately determined.

VIII. THE INFLUENCE OF OTHER ATOMS

We have devoted virtually all of the space in this article to discussion of the electronic structure of the copper-oxygen framework. Clearly this is the region of electronic interest, but there are at least two important roles played by the cations in these structures. First, we believe that the stability of a particular framework will be strongly influenced by the charge and size of the available cations via conventional "ionic" arguments. Our investigation of the stability of the alternative 1:2:3 structure of Fig. 18 stressed the importance of the choice of cation. Second, the electronegativity of the cations present in a given structure can affect in a subtle way the electronic structure of the copper oxide framework. In Sec. III we reported an axial-basal angle in the 1:2:3 compound from a calculation which included the yttrium atoms of the structure. A similar calculation without these atoms gave a poorer result (by 2°). We will describe the orbital influence of these other atoms in detail elsewhere, but this present result is sufficient to indicate a subtle control of this angle by the nature of the counterions. As we have already noted, the value of the geometrical parameter in this structure is important in controlling the size of plane-chain electron transfer.

IX. CONCLUSIONS

Perhaps the most important result of this work is the demonstration that many of the structural features of these systems may be interpreted in terms of conventional orbital-type arguments. Although we acknowledge that a complete description of these materials will only result by the addition of many-body terms to the band structure,

or via an alternative route, we feel that it is very important that the behavior on doping of parameters such as Cu-O distances and the relative stability of structural alternatives, such as the orthorhombic and tetragonal variants of the 2:1:4 compound, are readily understood in terms of conventional band structure arguments. In other words, whatever the ultimate electronic description of these systems and the nature of the superconducting mechanism, a significant component has to be integrated with well-established, nonexotic chemical principles. The fact that the orthorhombic-to-tetragonal transition in the 2:1:4 compound can be simply understood in terms of the degree of occupation of an x^2-y^2 band raises questions concerning the viewpoint that the holes in these superconductors lie formally on the oxygen atoms.[77] As we have mentioned above the orbital description of the x^2-y^2 band allows a significant oxygen contribution, but is this proposition consistent with this particular suggestion? A part of the problem to be addressed in the future is clearly the rationalization of viewpoints of the electronic structure of these systems derived from very different starting points.[78]

ACKNOWLEDGMENTS

This research was supported by The Office of Naval Research and also by The University of Chicago and the S.T.C. for High-Temperature Superconductivity. We would like to thank Professor K. Levin for many stimulating discussions.

APPENDIX

Both the band-structure calculations for the solid and the molecular-orbital calculations for CuO_x fragments were performed using the extended Hückel method. The parameters used are given in Table I. Typically, 16 **k** points were used in the irreducible wedge of the Brillouin zone for the solid-state calculations. For the computation of the charge transfer of Figs. 13 and 19, 24 points were used. Only the copper and oxygen atoms of these structures were used in the computations, except where explicitly stated.

[1]J. G. Bednorz and K. A. Muller, Z. Phys. B **64**, 189 (1986).
[2]M. K. Wu, J. R. Ashburn, C. J. Torng, P. H. Horn, R. L. Meng, L. Gao, Z. J. Huang, Y. Q. Wang, and C. W. Chu, Phys. Rev. Lett. **58**, 908 (1987).
[3]R. J. Cava, B. Batlogg, R. B. van Dover, D. W. Murphy, S. Sunshine, T. Siegrist, J. P. Remeika, E. A. Reitman, S. Zahurak, and G. P. Espinoza, Phys. Rev. Lett. **58**, 1676 (1987).
[4]R. J. Cava, R. B. van Dover, B. Batlogg, and E. A. Reitman, Phys. Rev. Lett. **58**, 408 (1987).
[5]C. N. R. Rao, P. Ganguly, A. K. Raychaudhuri, R. A. Mohanrram, and S. Sreedhar, Nature **326**, 856 (1987).
[6]ACS Symposium Series, No. 351, 1987, edited by D. L. Nelson, M. S. Whittingham, and T. F. George (ACS, Washington, D.C., 1987).
[7]ACS Symposium Series, No. 377, 1988, edited by D. L. Nelson and T. F. George (ACS, Washington, D.C., 1988).
[8]R. Hoffmann, *Solids and Surfaces* (Verlag Chemie, Weinheim, 1988).
[9]M.-H. Whangbo, R. Hoffmann, and R. B. Woodward, Proc. Roy. Soc. London **A366**, 23 (1979).
[10]J. K. Burdett, Progr. Solid State Chem. **15**, 173 (1984).
[11]A. W. Sleight, Ref. 6, p. 2.
[12]A. W. Sleight, Science **242**, 1519 (1988).
[13]L. F. Mattheiss, Phys. Rev. Lett. **58**, 1028 (1987).
[14]L. F. Mattheiss and D. R. Hamann, Solid State Commun. **63**, 395 (1987).
[15]J. Yu, A. J. Freeman, and J.-H. Xu, Phys. Rev. Lett. **58**, 1035 (1987).
[16]C. L. Fu and A. J. Freeman, Phys. Rev. B **35**, 8861 (1987).
[17]S. Massidda, J. Yu, A. J. Freeman, and D. D. Koelling, Phys. Lett. A **122**, 198 (1987).
[18]J. Yu, S. Massidda, A. J. Freeman, and D. D. Koelling, Phys. Lett. A **122**, 203 (1987).
[19]J. Redinger, A. J. Freeman, J. Yu, and S. Massidda, Phys. Lett. A **124**, 469 (1987).
[20]J. Redinger, J. Yu, A. J. Freeman, and P. Weinberger, Phys. Lett. A **124**, 463 (1987).
[21]J.-H. Xu, T. J. Watson-Yang, J. Yu, and A. J. Freeman, Phys. Lett. A **120**, 489 (1987).
[22]A. J. Freeman, J. Yu, and C. L. Fu, Phys. Rev. B **36**, 7111 (1987).
[23]P. W. Anderson, Science **235**, 1196 (1987).
[24]M.-H. Whangbo, M. Evain, M. A. Beno, and J. M. Williams, Inorg. Chem. **26**, 1829 (1987).
[25]M.-H. Whangbo, M. Evain, M. A. Beno, U. Geiser, and J. M. Williams, Inorg. Chem. **26**, 2566 (1987).
[26]M.-H. Whangbo, M. Evain, M. A. Beno, and J. M. Williams, Inorg. Chem. **26**, 1831 (1987).
[27]M.-H. Whangbo, M. Evain, M. A. Beno, and J. M. Williams, Inorg. Chem. **26**, 1832 (1987).
[28]R. Hoffmann, J. Chem. Phys. **39**, 1397 (1963).
[29]J. Gazo, I. B. Bersuker, J. Garaj, M. Kabesova, J. Kohout, H. Langfelderova, M. Melnik, M. Serator, and V. Velach, Coord. Chem. Rev. **19**, 253 (1976).
[30]J. K. Burdett, Inorg. Chem. **20**, 1959 (1981).
[31]J. K. Burdett and G. V. Kulkarni, J. Am. Chem. Soc. **110**, 5361 (1988).
[32]J. K. Burdett, *Molecular Shapes* (Wiley, New York, 1980).
[33]M. Gerloch and R. C. Slade, Ligand Field Parameters (Cambridge University Press, London, 1973).
[34]T. A. Albright, J. K. Burdett, and M.-H. Whangbo, *Orbital Interactions in Chemistry* (Wiley, New York, 1985).
[35]L. G. Vanquickenborne and A. Ceulemans, Inorg. Chem. **20**, 796 (1981).
[36]M. Gerloch, Inorg. Chem. **20**, 638 (1981).
[37]F. A. Cotton and C. B. Harris, Inorg. Chem. **6**, 369 (1967).
[38]R. Hoffmann, Angew. Chem. Int. Ed. Eng. **21**, 711 (1982).
[39]M. A. Beno, L. Soderhoin, D. W. Capone, D. G. Hinks, J. D. Jorgensen, I. K. Schuller, C. V. Serge, K. Zhang, and J. D. Grace, Appl. Phys. Lett. **51**, 57 (1987).
[40]R. J. Cava, B. Batlogg, C. H. Chen, E. A. Rietman, S. M.

Zahurak, and D. Werfer, Nature **329**, 423 (1987).
[41]Y. W. Yared, S. L. Miles, R. Bau, and C. A. Reed, J. Am. Chem. Soc. **99**, 7076 (1977).
[42]B. Raveau, C. Michel, M. Hervieu, and J. Provost, Rev. Solid State Science **2**, 115 (1988).
[43]See, for example, A. F. Wells, *Structural Inorganic Chemistry*, 5th ed. (Oxford University, New York, 1984), p. 1112.
[44]J. K. Burdett, Inorg. Chem. **24**, 2244 (1985).
[45]A. Simon, Angew, Chem. Int. Ed. Eng. **26**, 579 (1987).
[46]J. K. Burdett and S. Lee, J. Am. Chem. Soc. **107**, 3050 (1985); **107**, 3063 (1985); **107**, 3083 (1985).
[47]J. K. Burdett, Acc. Chem. Res. **21**, 189 (1988).
[48]J. K. Burdett, Struct. Bonding (Berlin) **65**, 29 (1987).
[49]See, for example, C. E. Moore, *Ionization Potentials and Ionization Limits Derived from Analyses of Optical Spectra*, Natl. Bur. Stand. Ref. Data Ser., Natl. Bur. Stand. (U.S.) Circ. No. 24 (U.S. GPO, Washington, D.C., 1970).
[50]L. F. Schneemeyer, J. K. Thomas, T. Siergrist, B. Batlogg, L. W. Rupp, R. L. Opila, R. J. Cava, and D. W. Murphy, Nature **335**, 421 (1988).
[51]G. Xiao, M. Z. Cieplak, D. Musser, A. Gavrin, F. H. Streitz, C. L. Chein, J. J. Rhyne, and J. A. Gotaas, Nature **332**, 328 (1988).
[52]R. J. Cava, B. Batlogg, K. M. Rabe, E. A. Reitman, P. K. Gallagher, and L. W. Rupp, Jr., Physica. C **156**, 523 (1988).
[53]S. D. Conradson and I. D. Raistrick, Science **243**, 1340 (1989).
[54]G. Xiao, M. Z. Cieplak, A. Garvin, F. H. Streitz, A. Bakhshai, and C. L. Chien, Revs. Solid State Sci. **1**, 323 (1987).
[55]A. Renault, J. K. Burdett, and J.-P. Pouget, J. Solid State Chem. **71**, 587 (1987).
[56]A. Ourmazd and J. C. H. Spence, Nature **329**, 426 (1987).
[57]A. Bianconi, A. Clozza, A. Congiu Castellano, S. Della Longa, M. de Santis, A. Dicicco, K. Garg, P. Deloug, A. Gargano, R. Giorgi, P. Lagarde, A. M. Frank, and A. Marcelli, *Proceedings of the Adriatic Research Conference on High Temperature Superconductors, Trieste, 1987*, edited by S. Lindquist (World Scientific, Singapore, 1987).
[58]Baudelet *et al.*, in Ref. 53.
[59]J. K. Burdett, G. V. Kulkarni, and K. Levin, Inorg. Chem. **26**, 3650 (1987).
[60]D. A. Papaconstantopoulos, W. E. Pickett, and M. J. DeWeert, Phys. Rev. Lett. **61**, 211 (1988).
[61]F. Izumi, H. Asano, T. Ishigaki, E. Muromachi, Y. Uchida, N. Watanabe, and N. Nishigaka, Jpn. J. Appl. Phys. **26**, L611 (1987).
[62]M. Onoda, S. Shamoto, M. Sata, and S. Hosoya, Jpn. J. Appl. Phys. **26**, L876 (1987).
[63]W. W. Schmidt, E. Salje, and W. Y. Liang, Philos. Mag. Lett. **58**, 173 (1988).
[64]J. A. Gardner, H. T. Su, A. G. McKale, S. S. Kao, L. L. Peng, W. H. Warnes, J. A. Sommers, K. Athreya, H. Franzen, and S.-J. Kim, Phys. Rev. B **38**, 11 317 (1988).
[65]H. W. Richardson, J. R. Wasson, and W. E. Hatfield, Inorg. Chem. **16**, 484 (1977).
[66]See, for example, R. A. Wheeler, M.-H. Whangbo, T. Hughbanks, R. Hoffmann, J. K. Burdett, and T. A. Albright, J. Amer. Chem. Soc. **108**, 2222 (1986).
[67]R. D. Shannon, Acta. Crystallogr. **A32**, 751 (1976).
[68]P. Marsh, R. M. Fleming, M. L. Mandich, A. M. DeSantolo, J. Kwo, M. Hong, and J. L. Martinez-Miranda, Nature **334**, 141 (1988).
[69]R. J. Cava, A. Santoro, D. W. Johnson, and W. W. Rhodes, Phys. Rev. B **35**, 6716 (1987).
[70]S. K. Sinha, Mater. Res. Bull. **13**, 24 (1988).
[71]R. C. Baetzold, Phys. Rev. B **38**, 11 304 (1988).
[72]J. K. Burdett, T. Hughbanks, G. J. Miller, J. W. Richardson, and J. V. Smith, J. Am. Chem. Soc. **109**, 3639 (1987).
[73]J. D. Jorgensen, H.-B. Schuttler, D. G. Hinks, D. W. Capone, K. Zhang, and M. B. Brodsky, Phys. Rev. Lett. **58**, 1024 (1987).
[74]R. J. Cava, B. Batlogg, J. J. Krajewski, L. W. Rupp, L. F. Schneemeyer, T. Siegrist, R. B. van Dover, P. Marsh, W. F. Peck, Jr., P. K. Gallagher, S. H. Glarum, J. H. Marshall, R. C. Farrow, J. V. Waszczak, R. Hull, and P. Trevor, Nature **336**, 211 (1988).
[75]C. Michel, M. Hervieu, M. M. Borel, A. Grandin, F. Deslandes, J. Provost, and B. Raveau, Z. Phys. B **68**, 421 (1987).
[76]Z. Z. Sheng, A. M. Hermann, E. El Ali, C. Almasan, J. Estrada, T. Datta, and R. J. Matson, Phys. Rev. Lett. **60**, 937 (1988).
[77]W. A. Goddard, Science **239**, 896 (1988).
[78]J. K. Burdett and G. V. Kulkarni, Chem. Phys. Lett. (to be published).